AEDC-TR-71-111

cy 2


# AN APPROXIMATE SOLUTION OF THE SUDDEN AREA EXPANSION FLOW PROCESS FOR FLOWS IN A ROTATING COORDINATE SYSTEM

J. W. Salvage

ARO, Inc.

August 1971



*ENGINEERING SUPPORT FACILITY*
*ARNOLD ENGINEERING DEVELOPMENT CENTER*
*AIR FORCE SYSTEMS COMMAND*
*ARNOLD AIR FORCE STATION, TENNESSEE*

# NOTICES

When U. S. Government drawings specifications, or other data are used for any purpose other than a definitely related Government procurement operation, the Government thereby incurs no responsibility nor any obligation whatsoever, and the fact that the Government may have formulated, furnished, or in any way supplied the said drawings, specifications, or other data, is not to be regarded by implication or otherwise, or in any manner licensing the holder or any other person or corporation, or conveying any rights or permission to manufacture, use, or sell any patented invention that may in any way be related thereto.

Qualified users may obtain copies of this report from the Defense Documentation Center.

References to named commercial products in this report are not to be considered in any sense as an endorsement of the product by the United States Air Force or the Government.

# AN APPROXIMATE SOLUTION OF THE SUDDEN AREA EXPANSION FLOW PROCESS FOR FLOWS IN A ROTATING COORDINATE SYSTEM

J. W. Salvage
ARO, Inc.

## FOREWORD

The work reported herein was sponsored by the Aerospace Research Laboratories, Office of Aerospace Research, under Program Element 6144501F, Sub-element 681307, Project 7065.

The results of the research presented were obtained by ARO, Inc. (a subsidiary of Sverdrup & Parcel and Associates, Inc.), contract operator of the Arnold Engineering Development Center (AEDC), Air Force Systems Command (AFSC), Arnold Air Force Station, Tennessee, under Contract F40600-72-C-0003. The research was conducted from December 1968 to December 1969 under ARO Project No. TW5001. The manuscript was submitted for publication on December 10, 1970.

The author, J. W. Salvage, is a research assistant at the University of Tennessee Space Institute (UTSI) assigned to ARO, Inc., under ARO subcontract to UTSI 70-25-TS/OMD.

The author is particularly indebted to Dr. M. K. Newman for his advice and counsel in solving the basic problem. The author is also grateful for the advice of Drs. C. E. Peters and A. J. Wennerstrom and for the assistance of several programmers who have worked on this problem: Mr. F. Worthy, Mr. M. M. Solomon, and Mr. K. W. Allen. Thanks are also due Mr. C. T. Carman for his support and Mr. J. R. Myers for his suggestions and assistance in assembling this report.

The research described in this report is aligned with, and considered as partial fulfillment of the requirements of a Masters Degree at UTSI.

This technical report has been reviewed and is approved.

Carlos Tirres
Captain, USAF
Research and Development Division
Directorate of Technology

Harry L. Maynard
Colonel, USAF
Director of Technology

## ABSTRACT

An approximate quasi-three-dimensional method of solution is described for the sudden area expansion flow process in the relative coordinate system under the assumptions of frictionless, adiabatic flow of a perfect gas. The objective was to determine the radial variation of the flow properties at the trailing edge of a rotor given the measured flow properties downstream of the rotor through use of the streamtube approximation. Results are derived from one configuration of the blunt trailing-edge supersonic compressor rotors tested at AEDC. The results were felt to be an unsatisfactory representation of the average flow conditions at the trailing edge, and it is shown that the reasons for this are relatable to neglecting the free turbulent shear flows occurring in the blade wakes in conjunction with neglecting the large radial secondary flows which apparently occur in the flow field of the rotor investigated. It is shown that the streamtube approximation can produce grossly inaccurate results when free turbulent shear is neglected on the streamtube boundaries. A proposal for continued work is also given.

## CONTENTS



## ILLUSTRATIONS

## APPENDIXES



## NOMENCLATURE

| | |
|---|---|
| A | Area |
| (A) | Surface area enclosing a region (R) |
| a | Local speed of sound |
| $\vec{a}_\theta$ | Tangential unit vector |
| $\vec{a}_r$ | Radial unit vector |
| b | Wake width |
| c | Chord length |

| | |
|---|---|
| $c_p$ | Specific heat at constant pressure |
| $c_v$ | Specific heat at constant volume |
| $d'_R( )$ | Streamline differential in the relative coordinate system |
| f | Force |
| $H'$ | Relative total enthalpy, $h + \frac{W^2}{2} - \frac{\Omega^2 r^2}{2}$ |
| K | A constant determining the radial variations of the blade angles |
| $\vec{k}$ | Axial unit vector |
| M | Mach number |
| $\mathfrak{M}$ | Moment of momentum vector |
| m | Mass flow rate |
| N | Rotor rotational speed, rpm |
| n | Number of blades |
| $\vec{n}$ | Unit vector normal to an incremental area |
| P | Total pressure |
| p | Static pressure |
| R | Gas constant (1715.608 $ft^2/sec^2$-°R) |
| (R) | Bounded region of the flow field |
| $R_P$ | Absolute total pressure ratio |
| r | Radial distance from the axis |
| s | Blade spacing, or surface length |
| T | Total temperature |
| t | Static temperature |
| $\vec{t}$ | Unit vector tangent to a surface element |
| th | Blade trailing-edge thickness |
| $\bar{u}$ | Local time-averaged velocity of mean motion |
| v | Volume |
| W | Velocity relative to the rotor or weight numbers used to determine the volume integrals of force due to Coriolis and Centripetal acceleration |
| y | Direction transverse to mean motion |

| | |
|---|---|
| $z$ | Axial distance |
| $\beta$ | Relative flow angle (yaw angle) measured in a tangential plane with respect to axial direction |
| $\beta$ | Blade angle measured in a tangential plane with respect to axial direction |
| $\gamma$ | Relative pitch angle measured in a plane perpendicular to a tangential plane with respect to the projection of the velocity vector onto the tangential plane |
| $\delta$ | Deviation angle, $\beta_2 - \beta_2'$ |
| $\epsilon$ | Virtual kinematic viscosity of turbulent flows |
| $\theta$ | Temperature correction factor for standardization defined as the ratio of the inlet absolute total temperature to the absolute total temperature of the Air Research and Development Command model sea-level atmosphere (519.3°R) |
| $\kappa$ | Ratio of specific heats, $c_p/c_v$ |
| $\kappa_1$ | Experimental constant for free turbulent flows |
| $\nu$ | Laminar kinematic viscosity |
| $\xi$ | Local angle of inclination of a surface of revolution to the axis of rotation |
| $\rho$ | Static density |
| $\tau$ | Shear stress |
| $\Omega$ | Magnitude of the rotational velocity |
| $\omega$ | Total pressure loss coefficient |

**SUBSCRIPTS**

| | |
|---|---|
| B | Boundary |
| e | A plane between the rotor trailing edge and the down stream measuring station 4 |
| f | Friction |
| geo | Geometric |
| h | Hub contour |
| I | Inner contour or boundary |

| | |
|---|---|
| 2 | Upstream of rotor |
| 3 | Free stream at blade trailing edge |
| $3'$ | Blade trailing edge surface |
| 4 | Axial measuring plane downstream of rotor; in particular, the traverse measurements at such a plane |
| 4R | Rake measurements at an axial measuring plane downstream of rotor |
| max | Maximum |
| min | Minimum |
| O | Outer contour or boundary |
| ref | Reference |
| SE | Sudden expansion |
| t | Tip, or rotor casing contour |
| w | Wall measurement |
| z | Axial direction |
| $\theta$ | Tangential direction |

**SUPERSCRIPTS**

| | |
|---|---|
| $'$ | Relative to rotor |
| $\bar{}$ | Average or overall |
| $\rightarrow$ | Vector quantity |

## SECTION I
## INTRODUCTION

The description of the three-dimensional flow in turbomachines is so mathematically complex and unrewarding to date that analysis of test data relating to turbomachines is often accomplished by assuming a model of the flow through a blade row and solving the design equations at stations between blade rows where there are no blade forces and where the analysis may be carried out in the absolute, or stationary, coordinate system (see Chapter III of Ref. 1, for example). As a model approximating the influences of a blade row, the analyst may choose pertinent cascade results and apply empirical correction factors to account for the stacking position of the blade element in the blade span and the additional frictional effects occurring in the blade end regions. Alternately, he may apply a completely mathematical model that satisfies the equations of fluid flow in two dimensions or one that basically originated from results of cascade testing or testing of rotors of similar design and then apply the additional three-dimensional correction factors.

Once the analyst has chosen his model, his results are completely relatable to that model. If the results agree with the experiment, then the model is considered good for that application, but the model may be limited only to that application. If the results only partially agree with experiment, the disagreement is attributable to influences which the analyst chose to neglect or could not account for.

This type of approach has its value to compressor or turbine designers although it may leave the real flow process in the rotor unexplained. At AEDC, under the sponsorship of ARL, several configurations of a high-reaction shock-in-rotor compressor rotor have been tested (Refs. 2 and 3). The blade element is of blunt trailing-edge design for the purpose of promoting supersonic constant-area diffusion to subsonic trailing-edge velocities while eliminating the starting difficulties generally associated with earlier designs of supersonic compressor blading (Ref. 4).

The process of supersonic constant-area diffusion cannot yet be handled by purely theoretical means. However, the process can be approximated because experimental results, such as those in Refs. 5 and 6, show that, if the passage length-to-height ratio is optimum, then the losses in the passage approach the losses of a single normal shock at an equivalent passage inlet Mach number. Thus, at least for optimum design, the trailing-edge flow conditions can be approximated.

Between the rotor trailing edge and the measuring station downstream of the rotor, unusually large mixing losses were anticipated because of the large trailing-edge thickness of the blading. The quasi-two-dimensional studies in Ref. 7 showed, however, that if the passage flow process behaved properly, then the Mach number at the trailing edge would be small enough so that the additional loss due to the abrupt increase in flow area would be of acceptable magnitude.

The results for the rotors tested at AEDC have been far below that expected of the blading, and the author has attempted in Ref. 8 to determine the cause of the poor performance through re-evaluation of the basic flow model. It was determined that the passage diffusion process was incomplete due either to the blade passage design or to the occurrence of separation or both of these. Therefore, the trailing-edge flow property distribution was uncertain since the basic passage flow model could not be effectively applied, and the real influence of the abrupt area increase at the trailing edge was unknown.

In an attempt to learn more about the flow property distribution at the trailing edge, and thereby more about the flow process in the rotor, it was decided to apply the flow model in a slightly unusual way. Rather than proceeding with the flow from upstream to downstream of the rotor as attempted in Refs. 9 and 10, the measured conditions upstream of the rotor were used to estimate shock loss alone, whereas the measured conditions downstream of the rotor were used to calculate the conditions at the trailing-edge plane. This report relates the consequences of using the measured downstream conditions in such a manner.

Initially, it was suspected that the quasi-two-dimensional theory (Ref. 7) would be limited, if not unsatisfactory, because considerable radial mass transfer was evident in the results of testing. Therefore, the quasi-three-dimensional technique presented in this report was developed both to allow radial shifting of stream surfaces in the flow field, a feature not allowed in the much simpler quasi-two-dimensional theory, and to allow determination of the radial variation of flow properties at the trailing edge.

Although the method presented in this report does permit these goals to be attained, the results must be considered quite unsatisfactory as a representation of the average flow properties at the trailing-edge plane. The method involves solution of the integral equations of motion in a relative, or rotating, coordinate system. Flow is assumed frictionless, and it is shown that this assumption is the primary reason for the unsatisfactory results. However, in contrast to general occurrences, shear stress is shown to be the determining factor throughout the flow

field, not just in the region of hub and tip casing walls. It is shown that the frictionless equations of motion will predict extremely large losses in relative total pressure when used in the manner described in this report, and it is further shown that free-turbulence, coupled with large radial secondary flows, is a reasonable explanation for the unsatisfactory results.

## SECTION II
## FORMULATION OF THE EQUATIONS FOR SUDDEN AREA EXPANSION WITH RADIAL VARIATION OF FLOW PROPERTIES

The blunt trailing-edge blading may be expected to have substantial additional losses in relative total pressure due to the viscous mixing process which occurs after the abrupt area increase at the trailing edge. The analysis in Ref. 7 develops quasi-two-dimensional equations to estimate the additional loss. The results indicate that the losses due to the sudden area expansion process are relatively small if the axial Mach number at the trailing-edge plane is not too close to unity. It has been indicated in Section I that the passage of the blunt trailing-edge compressor was designed as a constant-area diffuser to reduce supersonic inlet relative velocities to subsonic velocities at the trailing edge. Therefore, minimum sudden expansion loss depends on the proper design of the passage and requires a compromise between longer passage length to produce lower exit Mach numbers, thus increasing friction loss in the passage, and shorter passages to reduce machine weight, thereby increasing sudden expansion loss.

The quasi-two-dimensional analysis for the loss in relative total pressure due to the sudden area expansion process cannot determine the radial variation of loss; it can only give average values for the annulus. Furthermore, the quasi-two-dimensional theory requires that the radial velocity be zero for the entire process, but the test results have indicated that there is considerable radial change of stream surfaces through the wheel, especially at design speed. The use of the quasi-two-dimensional theory implies that all radial shift must occur within the rotor.

These considerations place strong limitations on the use of the quasi-two-dimensional theory; and a method has been derived which should determine the radial variation of important flow properties and the approximate position of streamlines at the axial location of the blade trailing edges. The method uses the integral flow equations for inviscid flow and provides solutions for the flow properties as a linear function

of radius over an arbitrary increment of radial annulus height. The method allows a tangential component of velocity to exist, but the solution does not determine tangential flow property variations; i. e., flow is still assumed axisymmetric so that the solutions are quasi-three-dimensional in nature, representing tangential averages at any radial station.

The method employs the integral equations of motion referred to a relative coordinate system rotating with the angular velocity of the compressor rotor. As discussed in Ref. 11, the choice of the relative coordinate system leads to equations involving volume integrals of the force due to Coriolis and centripetal accelerations. As stated in Ref. 11, these volume integrals generally cannot be evaluated without complete knowledge of the flow properties in the entire control volume. In some cases, flow property measurements have been made that allow an approximate calculation of the volume integrals. These cases are used to determine weighting factors applied to the surface integrals at entrance to and exit from the control volume such that the volume integrals determined by use of the weighting factors are equivalent to the volume integrals of the approximate calculations.

The use of the equations of motion in a rotating coordinate system should generally be limited to a region where every fluid element is participating in curvilinear motion imparted by the angular velocity of the wheel. In turbomachinery, its use should be limited to flow inside a rotating member where the force exerted by the blades generally dominates the frictional effects at the nonrotating surfaces that tend to change the transportational velocity of a fluid element. In the present application, the equations of motion for frictionless flow in a relative coordinate system are being applied to a region downstream of the rotor, but friction on the nonrotating surfaces of the casing walls could exert considerable influence on the solution because the flow property measurements are the result of a frictional flow field. In the present solution, frictional effects are ignored, and it is assumed that the inertial forces maintain the transportational motion of every fluid element.

It is, of course, possible to view the flow field in any coordinate system that may be chosen. The relative coordinate system was chosen because flow is more likely to be steady after the rotor in such a system. In the nonrotating, or absolute coordinate system, the flow may not be considered steady after the rotor. Thus, unsteady effects, as well as frictional effects, would have to be considered for complete solution of the problem in the absolute coordinate system.

## 2.1 DESCRIPTION OF THE PROBLEM

Consider a rotor of blunt trailing-edge blades and locate a rotating cylindrical coordinate system with its origin on the axis of the rotor and its axial unit vector ($\vec{k}$) pointed along the axis. The rotational velocity of the coordinate system ($\vec{\Omega}$) will be assumed to match the rotational velocity of the rotor. A positive value of the axial unit vector ($\vec{k}$) points in the positive direction of $\vec{\Omega}$ in the right-hand sense. A positive value of the tangential unit vector ($\vec{a}_\theta$) points in the direction of rotation. Defining the radial unit vector ($\vec{a}_r$) to point away from the axis when it is positive sets up the right-hand cylindrical coordinate system as shown in Fig. 1.

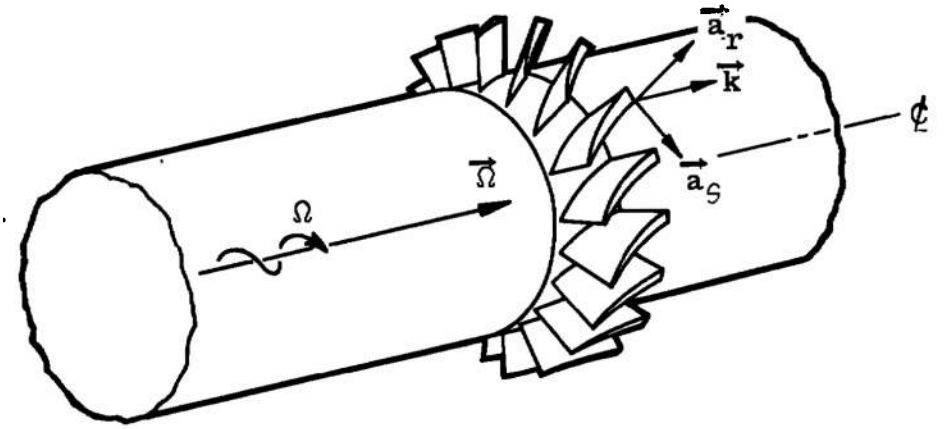


Fig. 1 A Three-Dimensional View of the Rotor

At a particular distance from the axis (r) a cylinder of radius r is made to intersect the blades. If this cylinder is then spread onto a plane, the blade profiles may be represented as shown in Fig. 2. This is the general representation of compressor blades in cascade. The blades are pictured with a spacing s, chord length c, and trailing-edge thickness th.

A plane perpendicular to the axis containing the blade leading edges in Fig. 1 is represented by the line $z = z_2$ in Fig. 2. A similar plane containing the blade trailing edges is represented by $z = z_3$ in Fig. 2. The plane $z = z_4$ in Fig. 2 is located far enough downstream so that complete mixing of the flow has occurred.

Figure 3 represents a plane containing the axis of the rotor intersecting the bounding walls of the rotor casing. This is the general representation of the compressor in the meridional plane. The curve C-C′ represents the generatrix of the compressor casing. The distance from the axis to the compressor casing ($r_t$) may be an arbirtary function

of z, the axial distance from the origin of the coordinate system. The curve D-D′ represents the generatrix of the compressor hub, and its distance from the axis ($r_h$) may be an arbitrary function of z.

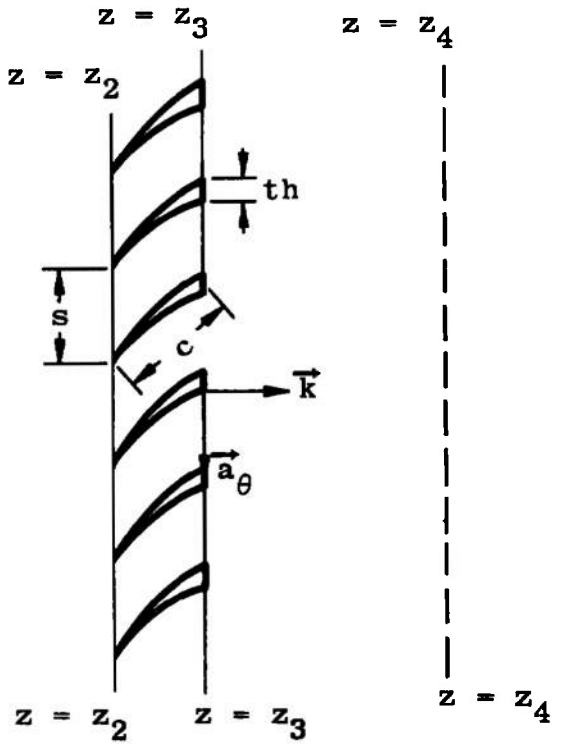


Fig. 2 The Cascade Representation of the Blading

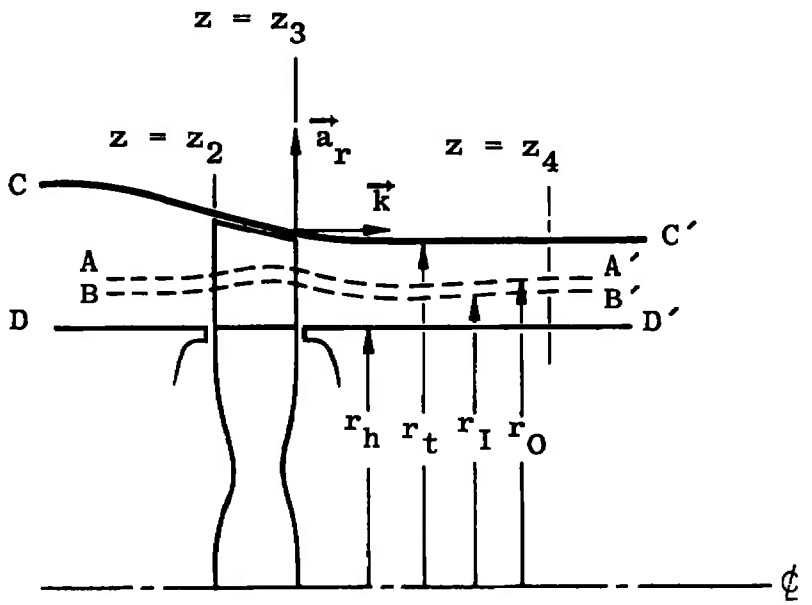


Fig. 3 A View of the Rotor in the Meriodional Plane

The region (R) of interest for the solution of the losses due to sudden area expansion will now be defined. The region (R) is enclosed by the planes $z = z_3$ and $z = z_4$ and the surfaces generated by C-C′ and D-D′ between these planes. The region will have a total surface area (A). Fluid flow may enter the region only through the surfaces area $A_3$, where $A_3$ is defined as the annulus area at $z = z_3$ excluding the area $A_3'$ occupied by the blade trailing edges. Fluid flow may leave the region only through the annulus area $A_4$ at $z = z_4$.

It is assumed that the flow through area $A_3$ at $z = z_3$ has not yet experienced the sudden area expansion and, also that it is in such a position that the blades may exert only an infinitesimal moment on the fluid.

The problem is to define the equations necessary to determine the relationship between the fluid properties at the planes $z = z_3$ and $z = z_4$.

Since the problem involves a great many unknowns and since the radial variation of some of the flow variables cannot be specified with certainty at the plane $z = z_3$, it is advantageous to divide the region (R) into a selected number of streamtubes. An example of one such streamtube is shown in Fig. 3 bounded by the generatrices A-A′ and B-B′. Then, with some confidence, radial variation of certain flow variables within each streamtube may be ignored. As an illustration, the adiabatic energy equation requires that the total enthalpy be constant along a streamline. In some cases, the assumption of constant total enthalpy within the entire region may be crude. However, if the region is divided so that radial variation of total enthalpy is small within each streamtube, accuracy may be improved.

The streamtube approximation is inaccurate whenever there is net mass transfer between streamtubes; i.e., secondary flows within the region. This represents a limitation in the solution of the problem.

## 2.2 ASSUMPTIONS FOR THE SIMPLIFICATION OF THE EQUATIONS

In order to simplify the equations, the following assumptions were made:

1. The fluid is a perfect gas. This assumption allows the use of the equation of state for a perfect gas,

$$p = \rho R t \tag{1}$$

where p is the static pressure, $\rho$ is the density, t is the static temperature, and R is the gas constant. Furthermore, the specific heat at constant pressure ($c_p$) is constant so that the ratio of specific heats ($\kappa$) is a constant which, thereby, tends to simplify computation.

2. The weight of the fluid in the region (R) is negligible. In comparison to the inertial forces, the weight of the gas is usually quite small, and this assumption allows a volume integral to be neglected.

3. Flow is steady. It is necessary to consider a rotating coordinate system for rotor flows in order to efficiently use this approximation. The integral equations to be applied to this problem contain volume integrals of unsteady effects requiring complete knowledge of the flow at every point in the region at every instant of time. It is usually not experimentally possible to evaluate this integral for the type of problem under consideration. Time averaged values of the flow properties reduce the error in this assumption.

4. Flow is adiabatic and frictionless. The energy equation will normally include the heat generated by friction along the path of a fluid particle if the flow is assumed steady and if heat transfer to the boundaries of the region is ignored when it is assumed that the heat due to friction is immediately and entirely dispersed throughout the fluid element. However, the mathematical complexity of including the frictional term in the momentum equation requires the total neglection of friction for the present calculations.

5. Flow is axisymmetric throughout the region (R). This assumption implies that there is no variation of the flow properties in the tangential ($\vec{a}_\theta$) direction at any particular axial position (z) and radial distance from the axis (r). If the plane $z = z_4$ is far enough downstream, this assumption produces very little inaccuracy at this station; however, because of the unusually large thickness of the blade trailing edges, this assumption becomes progressively poorer as the plane $z = z_3$ is approached.

   The plane at $z = z_3$ is essentially made up of two different types of surfaces that partially bound the region (R). One is the effective surface of the blade trailing edges comprised of the actual trailing-edge surface area and the

portion of the blade surface boundary layer that is intersected by the plane $z = z_3$. The area of this surface was termed earlier $A_3'$. By assumption, no flow may enter the region through this surface, but secondary flows, perhaps caused by centrifugal forces for instance, could conceivably cause components of the velocity to exist. The other type of surface at $z_3$ comprises the area between the blades through which flow enters the region (R), and it was earlier termed $A_3$. In general, sizable tangential variation of all flow properties may be expected in the $z_3$ plane, particularly if the blades are cambered, although one might expect these variations to be periodic from blade to blade if the flow relative to the blades is steady. The equations used to describe the sudden expansion process will account for the assumption that the velocity is identically zero over the surface $A_3'$, whereas the assumption of axial symmetry will be used to neglect any tangential variation over the surface $A_3$. These assumptions lead to equations that still contain terms which allow possible differences between the static pressures on the surface $A_3'$ and $A_3$.

The results of the calculation presented in this report are derived from equations which assume that the static pressure on the blade trailing-edge surface and the static pressure in the free stream are identical. However, some reports (for example, Ref. 12) indicate that there may be considerable difference between these pressures, and the proper equations accounting for this are presented. In this case, a relationship of the form

$$p_3' = p_3 f(M_{3z}', A_4/A_3, \kappa) \tag{2}$$

is required where $p_3'$ is the pressure on the trailing-edge surfaces, $p_3$ is the free-stream static pressure, and $f(M_{3z}', A_4/A_3, \kappa)$ may be an empirically determined function of the free-stream axial Mach number ($M_{3z}'$), the flow area ratio ($A_4/A_3$), and the ratio of specific heats ($\kappa$).

6. Secondary flows are neglected. Such an assumption is likely to be unrealistic in fluid flow as complicated as that in turbomachines. By way of example, consider

the space behind a blade trailing edge. In all likelihood, such a region contains an unusually large amount of low energy boundary layer material compared with blading of more conventional design. This low energy fluid can be more easily centrifuged outward to collect at the casing than the main stream flow. This particular type of secondary flow is probably inherent in the overall picture of flow with the blunt trailing-edge blading.

Various other types of secondary flows are described in Chapter XV of Ref. 1. Experimental evidence related in Ref. 1 indicates that wheels of high hub-to-tip radius ratios may be expected to reduce secondary flows. In any case, only qualitative analysis from experimental data for secondary flows is available to date because of the mathematical complexity of the problem.

## 2.3 THE EQUATIONS FOR A ROTATING COORDINATE SYSTEM

The following is a list of the equations applied for solution of the sudden area expansion phenomenon. For the most part, they are taken directly from Ref. 11. In review, the derivation of these basic equations hypothesized a flow that is representable by field properties that are continuous and continuously differentiable. The angular velocity of rotation has been assumed constant; separation at the planes of entrance to and exit from the control volume is assumed not to occur; and flow may not both enter and leave the control volume through the same open surface area.

### 2.3.1 Momentum Equation

The integral momentum equation for steady relative flow, neglecting friction and the weight of the gas, is

$$\int_{(A_4)} \vec{W}_4 \, dm_{A_4} - \int_{(A_3)} \vec{W}_3 dm_{A_3} = \int_{(A)} -\vec{n} p dA - \int_{(R)} \rho \vec{\Omega} \times (2\vec{W} + \vec{\Omega} \times \vec{r}) \, dv \qquad (3)$$

where $dm_{A_i}$ is the absolute value of the increment of the mass flow rate defined by

$$dm_{A_i} = \rho_i \vec{n} \cdot \vec{W}_i | dA_i \qquad (4)$$

where $\rho$ is the density, $\vec{n}$ the unit vector normal to the element of surface area $dA_i$, and $\vec{W}_i$ is the relative velocity given in cylindrical coordinates by

$$\vec{W}_i = \vec{a}_r W_{r_i} + \vec{a}_\theta W_{\theta i} - \vec{k} W_{z_i} \tag{5}$$

In Eq. (3), the areas $A_3$ and $A_4$ are the areas through which the fluid, respectively, enters and leaves the region (R). The region (R) is bounded by a surface of total area (A). By convention, the unit normal vector ($\vec{n}$) points away from the region (R) so that the negative sign in the integral of the static pressure (p) indicates that the normal stress is exerted on the surface element dA by the surroundings. In general, the final volume integral of Eq. (3) for the Coriolis acceleration ($2\vec{\Omega} \times \vec{W}$) and the centripetal acceleration ($\vec{\Omega} \times (\vec{\Omega} \times \vec{r})$) cannot be evaluated accurately because of lack of sufficient flow measurements within the region.

### 2.3.2 Continuity Equation

The continuity equation may be written in integral form for steady flow in the relative coordinate system as

$$\int_{(A_3)} dm_{A_3} = \int_{(A_4)} dm_{A_4} \tag{6}$$

where $dm_{A_i}$ is given in Eq. (4).

### 2.3.3 Energy Equation

The energy equation for steady, adiabatic flow in a rotating coordinate system is

$$d'_R H' = 0$$

where $d'_R( )$ represents the change along the path of a fluid particle in the rotating coordinate system and where $H'$ is the relative total enthalpy. For a perfect gas, this leads to

$$T'_3 = T'_4 + \frac{\kappa - 1}{2\kappa R} \Omega^2 (r_3^2 - r_4^2)$$

The streamtube approximation is used in approximating an average value of $T_3'$ in each streamtube based on the mass averaged value of $T_4'$, the streamtube center at $z_4$, and an arithemetic average of the inner and outer boundary radii at $z_3$.

### 2.3.4 First Moment of Momentum

The axial component of the first moment of momentum for steady, frictionless flow of a weightless gas in a rotating coordinate system is given by

$$\mathfrak{M}'_z = \int_{(A_3)} \vec{k} \cdot \vec{r}_3 \times W_3 dm_{A_3} - \int_{(A_4)} \vec{k} \cdot \vec{r}_4 \times \vec{W}_4 \, dm_{A_4} - \int_{(R)} \vec{k} \cdot \vec{r} \times [\rho\vec{\Omega} \times (2\vec{W} + \vec{\Omega} \times \vec{r})] \, dv \tag{7}$$

If no force is exerted in the tangential direction, this equation equals zero.

## 2.4 DERIVATION

The problem which now remains is the rearrangement of the above equations into the most useful form. To do this, several additional relationships are necessary. The relative Mach number vector ($\vec{M}'$) is given by

$$\vec{M} = \frac{\vec{W}}{a}$$

where

$$a = \sqrt{\kappa R t}$$

Using the isentropic relation (Ref. 11) gives

$$\frac{T}{t} = 1 + \frac{\kappa - 1}{2} M^2$$

The static temperature may be replaced by the relative total temperature ($T'$) when the Mach number in the above relation is considered the relative Mach number ($M'$). Then the local speed of sound is given by

$$a = \frac{\sqrt{\kappa R T'}}{\left(1 + \frac{\kappa - 1}{2} M'^2\right)^{1/2}}$$

so that the relative velocity ($\vec{W}$) may be replaced by

$$\vec{W} = \frac{\vec{M}' \sqrt{\kappa R T'}}{\left(1 + \frac{\kappa - 1}{2} M'^2\right)^{1/2}} \tag{8}$$

It is now convenient to define the geometry of the surfaces bounding the region (R). The effective thickness of a blade at the trailing

edge (th) may, in general, be a function of the radial distance from the axis. If th is considered the arc length at a particular radius r, then the angle intercepted by this thickness is th/r. The cross-sectional area at the trailing edge occupied by a single blade is then

$$A = \int_{r_{3h}}^{r_{3t}} \int_{0}^{th/r} r\,d\theta\,dr$$

$$= \int_{r_{3h}}^{r_{3t}} th\,dr$$

where the subscript 3 indicates the plane at $z = z_3$, the plane of the trailing edge, t implies the tip or outer casing, and h implies the hub or inner casing. Then for n blades the incremental area at the trailing edge ($dA_3'$) is given by

$$dA_3' = n\,th\,dr \tag{9}$$

For the assumption of axisymmetric flow, the element of area at $z = z_3$ through which fluid may pass ($dA_3$) is given by

$$dA_3 = (2\pi r - n\,th)dr \tag{10}$$

The element of surface area $A_4$ at $z = z_4$ is

$$dA_4 = 2\pi r dr \tag{11}$$

for axisymmetric flow.

To the present point in the derivation, the control volume has been considered that volume bounded by the axisymmetric surfaces of the inner and outer casing walls, the plane of the rotor blade trailing edges ($z_3$), and the downstream measuring plane ($z_4$). The streamtube approach is next applied to divide this control volume into smaller regions. This procedure is necessary to allow the linear representations of the flow properties in each streamtube to be sufficiently accurate and to reduce inaccuracy in the integration of the energy equation. At the downstream measuring plane, several stream surface locations may be determined by use of the measurements at this station in conjunction with the continuity equation. It is assumed in the present application that the hypothetical stream surfaces of each streamtube are parts of right circular cones between measuring planes and the plane of the blade trailing edges. A significant portion of the problem involves locating the stream surfaces at the blade trailing edge plane. It is assumed that

there is no net mass transfer across the stream surfaces. Two examples of such stream surface configurations are shown in Fig. 4 as a cross-sectional view containing the rotor axis. Figure 4 (top) shows the boundaries of a streamtube that might occur when there are no extra measurements at an axial plane between the rotor trailing edge plane and the downstream measuring plane. Figure 4 (bottom) shows a possible configuration when the extra measuring plane is included for determination of the weight numbers for the volume integrals (see Section 2.8).

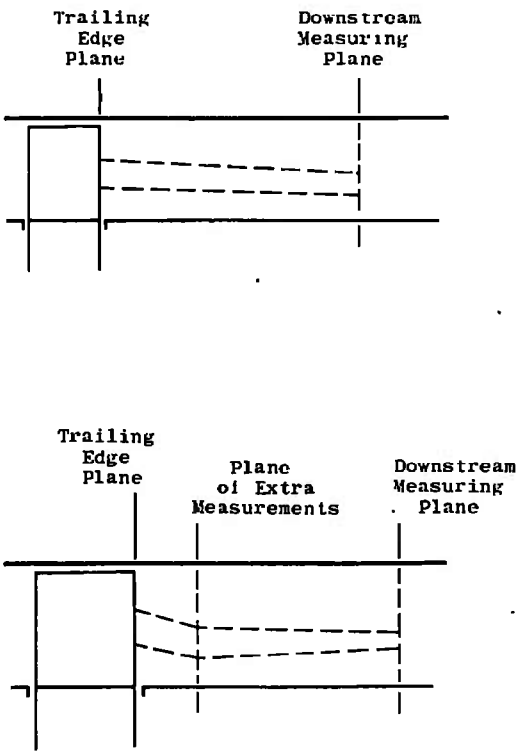


**Fig. 4 Examples of Arbitrary Stream Surface Configurations**

In order to define the elements of surface area for the axisymmetric stream surface bounding the streamtubes, it should be recalled that curves like A-A′, B-B′, C-C′ and D-D′ in Fig. 3 represent the generatrices of axisymmetric surfaces. A streamtube like that bounded by A-A′ and B-B′ in Fig. 3 has one surface boundary (B-B′) that is closer to the axis of generation which will be termed the inner boundary (subscript I) and one surface boundary (A-A′) that is farther away from the axis of generation which will be termed the outer boundary (subscript O). The elements of area for the inner and outer streamtube boundaries are given by, respectively,

$$dA_I = 2\pi r_I(z)\ ds_I$$

and

$$dA_O = 2\pi r_O(z)\, ds_O$$

where, in general, $r_I$ and $r_O$ may be arbitrary functions of z and ds is the element of length between $z = z_3$ and $z = z_4$ in a plane containing the axis. For a straight line, the length elements ds may be given by

$$ds_I = \frac{dz}{\cos \xi_I}$$

$$ds_O = \frac{dz}{\cos \xi_O}$$

where $\xi$ is the angle of a tangent to the surface measured with respect to the axis in a plane containing the axis. The elements of area of the the streamtube surface boundaries then become

$$dA_I = \frac{2\pi r_I(z)\, dz}{\cos \xi_I} \tag{12}$$

and

$$dA_O = \frac{2\pi r_O(z)\, dz}{\cos \xi_O} \tag{13}$$

The unit normal vectors to each element of the total surface area (A) may now be determined. First, the planes $z = z_3$ and $z = z_4$ are perpendicular to the axis of the rotor; therefore, the normals to these surfaces are parallel to the unit vector $\vec{k}$. The unit normal vectors point away from the region (R) so that the unit normal vector at $z = z_3$ is equivalent to $-\vec{k}$. Similarly at $z = z_4$, the unit normal vector equals $+\vec{k}$. To designate the components of the vectors normal to $dA_I$ and $dA_O$ consider Fig. 5. The sign of the angle $\xi$ which the wall makes with positive axial direction is positive if $r_4 > r_3$ for $z_4 > z_3$ and negative if $r_4 < r_3$ for $z_4 > z_3$. Figure 5a shows two possible local orientations of the inner boundary generatrix. The normal to the inner streamtube boundary is given in both cases by

$$\vec{n} = \vec{k} \sin \xi_I - \vec{a}_r \cos \xi_I \tag{14}$$

Similarly, Fig. 5b shows two possible local orientations of the outer boundary generatrix. The normal to the outer streamtube boundary is given in both cases by

$$\vec{n} = \vec{a}_r \cos \xi_O - \vec{k} \sin \xi_O \tag{15}$$

The element of volume for the region (R) is given by

$$dV = 2\pi r \, dr \, dz \tag{16}$$

for axisymmetric flow where r may be a function of z.

The various vector products occurring in Eqs. (3) and (7) may be evaluated using Eq. (5), the relation

$$\vec{r} = \vec{a}_r r + \vec{k} z$$

and the fact that $\vec{\Omega} = \vec{k}\Omega$. Then the following relations result:

$$\left.\begin{aligned}
&\vec{\Omega} \times \vec{W} = -\vec{a}_r \Omega W_\theta - \vec{a}_\theta \Omega W_r \\
&\vec{\Omega} \times (\vec{\Omega} \times \vec{r}) = -\vec{a}_r \Omega^2 r \\
&\vec{k} \cdot \vec{r} \times \vec{W} = r W_\theta \\
&\vec{k} \cdot \vec{r} \times [\rho\vec{\Omega} \times (2\vec{W} + \vec{\Omega} \times \vec{r})] = 2\rho\Omega r W_r
\end{aligned}\right\} \tag{17}$$

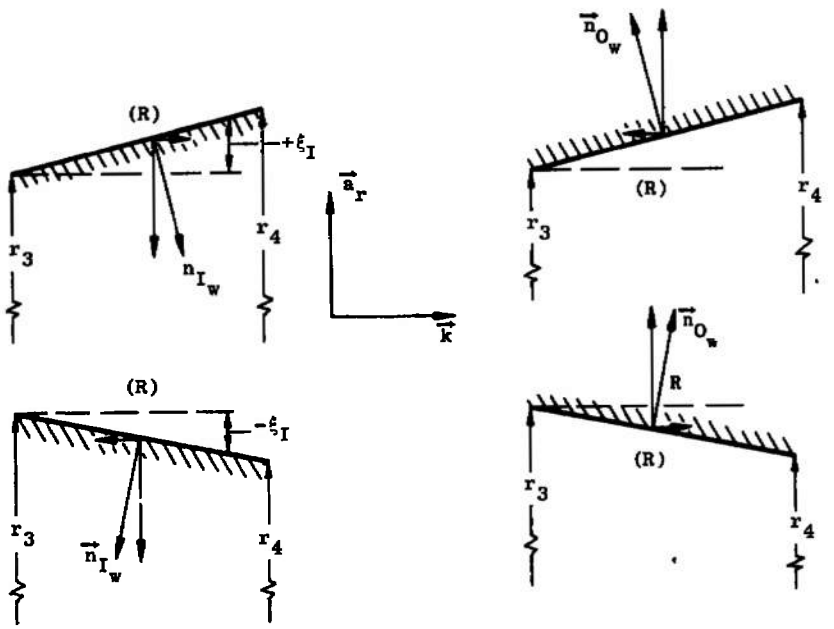


a. Inner Boundary

b. Outer Boundary

**Fig. 5 Geometric Relation of the Vectors Normal to the Axisymmetric Stream Surfaces**

The following relations are derived from Fig. 6 and allow substitution for the components of the relative velocity.

$$\left.\begin{aligned}
W_z &= W \cos\gamma \cos\beta \\
W_r &= W \sin\gamma \\
W_\theta &= -W \cos\gamma \sin\beta
\end{aligned}\right\} \tag{18}$$

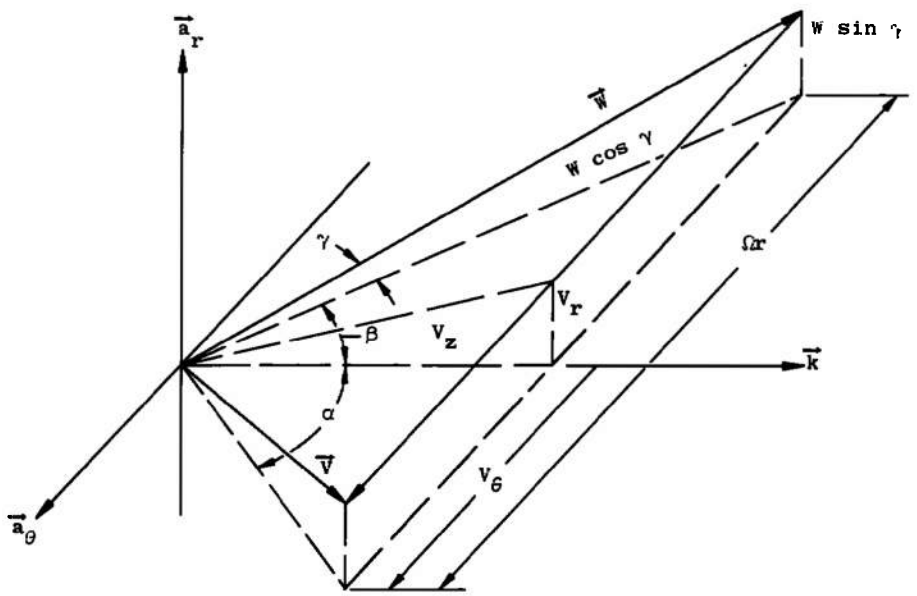


**Fig. 6 The Three-Dimensional Velocity Triangle**

By using Eqs. (1), (4), and (5) and relations in Eqs. (8) to (18), it is possible to rearrange Eqs. (3), (6), and (7) to the following form

Radial Component of the Momentum Equation

$$\int_{r_{3I}}^{r_{30}} p_3 M_3'^2 \sin\gamma_3 \cos\gamma_3 \cos\beta_3 \left(1 - \frac{n\,th}{2\pi r}\right) rdr = A' + B' + R_1' + R_2' \quad (19)$$

where

$$A' \equiv \int_{r_{4I}}^{r_{40}} p_4 M_4'^2 \sin\gamma_4 \cos\gamma_4 \cos\beta_4 \, rdr \quad (20)$$

$$B' \equiv \frac{1}{\kappa} \int_{z_3}^{z_4} (p_{OR_O} - p_{IR_I})\, dz \quad (21)$$

$$R_1' \equiv \frac{\Omega}{\pi\sqrt{\kappa R}} \int_{(R)} \frac{pM'}{\sqrt{T'}} \left(1 + \frac{\kappa - 1}{2} M'^2\right)^{1/2} \cos\gamma \sin\beta \, dv \quad (22)$$

$$R_2' \equiv -\frac{\Omega^2}{2\pi\kappa R} \int_{(R)} \frac{p}{T'} \left(1 + \frac{\kappa - 1}{2} M'^2\right) rdv \quad (23)$$

Tangential Component of the Momentum Equation

$$\int_{r_{3I}}^{r_{30}} p_3 M_3'^2 \cos^2 \gamma_3 \sin \beta_3 \cos \beta_3 \left(1 - \frac{n\,th}{2\pi r}\right) rdr = C' + R_3' \tag{24}$$

where

$$C' \equiv \int_{r_{4I}}^{r_{40}} p_4 M_4'^2 \cos^2 \gamma_4 \sin \beta_4 \cos \beta_4 \; rdr \tag{25}$$

$$R_3' \equiv \frac{-\Omega}{\pi\sqrt{\kappa R}} \int_{(R)} \frac{pM'}{\sqrt{T'}} \left(1 + \frac{\kappa - 1}{2} M'^2\right)^{1/2} \sin \gamma \, dv \tag{26}$$

Axial Component of the Momentum Equation

$$\int_{r_{3I}}^{r_{30}} p_3 \left(M_3'^2 \cos^2 \gamma_3 \cos^2 \beta_3 + \frac{1}{\kappa}\right)\left(1 - \frac{n\,th}{2\pi r}\right) rdr = D' + E' + F' \tag{27}$$

where

$$D' \equiv \int_{r_{4I}}^{r_{40}} p_4 \left(M_4'^2 \cos^2 \gamma_4 \cos^2 \beta_4 + \frac{1}{\kappa}\right) rdr \tag{28}$$

$$E' \equiv \frac{1}{\kappa} \int_{z_3}^{z_4} (p_{Ir_I} \tan \xi_I - p_{O r_O} \tan \xi_O) \, dz \tag{29}$$

$$F' \equiv -\frac{1}{\kappa} \int_{r_{3I}}^{r_{30}} p_3' \frac{n\,th}{2\pi r} \; rdr \tag{30}$$

Continuity Equation

$$\frac{1}{\sqrt{T_3'}} \int_{r_{3I}}^{r_{30}} p_3 M_3' \cos \gamma_3 \cos \beta_3 \left(1 + \frac{\kappa - 1}{2} M_3'^2\right)^{1/2} \left(1 - \frac{n\,th}{2\pi r}\right) rdr = \frac{G'}{\sqrt{T_4'}} \tag{31}$$

where

$$G' \equiv \int_{r_{4I}}^{r_{40}} p_4 M_4' \cos \gamma_4 \cos \beta_4 \left(1 + \frac{\kappa - 1}{2} M_3'^2\right)^{1/2} rdr \tag{32}$$

Axial Component of the Law of Moment of Momentum

$$\int_{r_{3I}}^{r_{3O}} p_3 M_3'^2 \cos^2\gamma_3 \sin\beta_3 \cos\beta_3 \left(1 - \frac{n\,th}{2\pi r}\right) r^2 dr = H' + R_4' \tag{33}$$

where

$$H' \equiv \int_{r_{4I}}^{r_{4O}} p_4 M_4'^2 \cos^2\gamma_4 \sin\beta_4 \cos\beta_4 r^2\, dr \tag{34}$$

$$R_4' \equiv \frac{-\Omega}{\pi\sqrt{\kappa R}} \int_{(R)} \frac{pM'}{\sqrt{T'}} \left(1 + \frac{\kappa - 1}{2} M'^2\right)^{\frac{1}{2}} \sin\gamma\, r\, dv \tag{35}$$

Equations (19), (24), (27), (31), and (33) describe the process of sudden area expansion for a rotor of blunt trailing-edge blading under the present assumptions. In order to actually solve the equations, it is necessary to make further assumptions and to select five particular quantities to be obtained by the solution. The following sections deal with these problems.

## 2.5 FURTHER ASSUMPTIONS TO SIMPLIFY THE PROBLEM

### 2.5.1 Assumption 1

The quantities $A'$ of Eq. (20), $C'$ of Eq. (25), $D'$ of Eq. (28), $G'$ of Eq. (32), and $H'$ of Eq. (34) involve only the properties of the flow at the plane $z = z_4$. These quantities may be evaluated numerically from measurements at the $z_4$ plane.

For the specific case of the present analysis, it is assumed that the radial component of Mach number is identically zero at $z = z_4$; i.e., $\gamma_4 \equiv 0$ (see Eq. (18)). Measurements were obtained under this assumption, and in Ref. 8, it was demonstrated that neglecting radial velocity produces only small errors at this plane.

### 2.5.2 Assumption 2

The quantities $B'$ of Eq. (21) and $E'$ of Eq. (29) involve the pressure on the streamtube bounding surfaces and the shape of these surfaces between $z_3$ and $z_4$. In general, neither of these is fully known, and therefore, they must be approximated.

Static pressure is measured only on the casing walls; but with the assumptions that static pressure varies linearly in the radial direction and that the stream surfaces form portions of right circular cones, it is possible to separate the functions into integrals that remain constant for all streamtubes and coefficients of these integrals that are determined by a streamtube's location and geometry. The following discussion shows the exact procedure leading to this simplification.

It will be assumed that the surfaces of a streamtube form a portion of a right cone which has an axis coinciding with the axis of the rotor. This means that, in the representation of Fig. 3, the streamtube has straight lines denoting stream surface shape between planes $z = z_3$ and $z = z_4$. Then radial distance of a stream surface at any axial location z, $z_3 < z < z_4$, is given by

$$r_i(z) = r_{4i} - (r_{4i} - r_{3i}) \frac{z_4 - z}{z_4 - z_3}, \quad i = \text{I or O} \tag{36}$$

The slope in the z direction of a stream surface is approximated by

$$\tan \xi_i = \frac{r_{4i} - r_{3i}}{z_4 - z_3}, \quad i = \text{I or O} \tag{37}$$

The static pressure is usually measured at static taps positioned along the solid boundaries. The variation of static pressure from inner to outer walls is assumed linear. Then for a particular axial station (z), the variation of static pressure with radius is given by

$$p(r, z) = p_{1w}(z) + [p_t(z) - p_h(z)] \frac{r - r_h(z)}{r_t(z) - r_h(z)} \tag{38}$$

where $r_h(z)$ and $r_t(z)$ are, respectively, the hub and tip casing wall radii at the particular axial station z, and where $p_h(z)$ and $p_t(z)$ are the static pressures measured at the hub and tip walls, respectively, for the particular axial station z. Since it is of particular interest to know the static pressure on the stream surface, the streamtube surface radius of Eq. (36) must be substituted for r in Eq. (38). Then the static pressure on the streamtube surface i (= O or I) at the particular axial position z is given by

$$p_i(z) = p_h(z) + [p_t(z) - p_h(z)] \left[\frac{r_{4_1} - r_h(z)}{r_t(z) - r_h(z)}\right] - [p_t(z) - p_h(z)] \left[\frac{z_4 - z}{z_4 - z_3}\right] \left[\frac{r_{4_1} - r_{3_1}}{r_t(z) - r_h(z)}\right] \tag{39}$$

Substitution of Eqs. (36) and (39) into Eq. (21) leads to the following representation of B′:

$$B' = (r_{40} - r_{41})\,B_1' + (r_{40}^2 - r_{41}^2)\,B_2' + 2\,(r_{30}r_{40} - r_{31}r_{41})\,B_3' + (r_{30} - r_{31})\,B_4' + (r_{30}^2 - r_{31}^2)\,B_5' \tag{40}$$

where

$$B_1' \equiv \frac{1}{\kappa}\int_{z_3}^{z_4}\left(1 - \frac{z_4 - z}{z_4 - z_3}\right)\left(p_h - \frac{p_t - p_h}{r_t - r_h}\,r_h\right)dz \tag{41}$$

$$B_2' \equiv \frac{1}{\kappa}\int_{z_3}^{z_4}\left(1 - \frac{z_4 - z}{z_4 - z_3}\right)^2\left(\frac{p_t - p_h}{r_t - r_h}\right)dz \tag{42}$$

$$B_3' \equiv \frac{1}{\kappa}\int_{z_3}^{z_4}\left(\frac{z_4 - z}{z_4 - z_3}\right)\left(1 - \frac{z_4 - z}{z_4 - z_3}\right)\left(\frac{p_t - p_h}{r_t - r_h}\right)dz \tag{43}$$

$$B_4' \equiv \frac{1}{\kappa}\int_{z_3}^{z_4}\left(\frac{z_4 - z}{z_4 - z_3}\right)\left(p_h - \frac{p_t - p_h}{r_t - r_h}\,r_h\right)dz \tag{44}$$

$$B_5' \equiv \frac{1}{\kappa}\int_{z_3}^{z_4}\left(\frac{z_4 - z}{z_4 - z_3}\right)^2\left(\frac{p_t - p_h}{r_t - r_h}\right)dz \tag{45}$$

Similarly, substitution of Eqs. (36), (37), and (39) into Eq. (29) yields

$$E' = (r_{41}^3 - r_{40}^3)\,\frac{B_2'}{z_4 - z_3} + (r_{41}^2 - r_{40}^2)\,\frac{B_1'}{z_4 - z_3} + (r_{30}^3 - r_{31}^3)\,\frac{B_5'}{z_4 - z_3} + (r_{30}^2 - r_{31}^2)\,\frac{B_4'}{z_4 - z_3} + (r_{30}^2 r_{40} - r_{31}^2 r_{41})\,\frac{E_1'}{z_4 - z_3} + (r_{30}r_{40}^2 - r_{31}r_{41}^2)\,\frac{E_2'}{z_4 - z_3} + (r_{30}r_{40} - r_{31}r_{41})\,\frac{E_3'}{z_4 - z_3} \tag{46}$$

where B′1, B′2, B′4, and B′5 are given, respectively, by Eqs. (41), (42), (44), and (45) and where

$$E_1' \equiv \frac{1}{\kappa}\int_{z_3}^{z_4}\left(\frac{z_4 - z}{z_4 - z_3}\right)\left(2 - 3\,\frac{z_4 - z}{z_4 - z_3}\right)\left(\frac{p_t - p_h}{r_t - r_h}\right)dz \tag{47}$$

$$E_2' \equiv \frac{1}{\kappa}\int_{z_3}^{z_4}\left(1 - \frac{z_4 - z}{z_4 - z_3}\right)\left(1 - 3\,\frac{z_4 - z}{z_4 - z_3}\right)\left(\frac{p_t - p_h}{r_t - r_h}\right)dz \tag{48}$$

$$E_3' \equiv \frac{1}{\kappa}\int_{z_3}^{z_4}\left(1 - 2\,\frac{z_4 - z}{z_4 - z_3}\right)\left(p_h - \frac{p_t - p_h}{r_t - r_h}\,r_h\right)dz \tag{49}$$

It should be noted that the integrals represented by $B'_i$, i = 1, ..., 5, and $E'_i$, i = 1, 2, 3, involve only the measured values of the wall static pressure and the annulus wall radii. Therefore, these quantities may be integrated without knowledge of the streamtube configurations and considered constants in obtaining the solution. However, since evaluation of the integrals requires knowledge of the annulus wall static pressure at the plane of the trailing edge, a particular problem arises at hub wall where no wall static pressure may be measured in practice. In the present application, the other measured static pressures along the hub wall are used to extrapolate for the missing value. It is felt that since the integrals are based on several actual measured values, little error is involved in this necessary approximation.

### 2.5.3 Assumption 3

The volume integrals $R'_1$ of Eq. (22), $R'_2$ of Eq. (23), $R'_3$ of Eq. (26), and $R'_4$ of Eq. (35) require, in general, complete knowledge of the flow at every point within the region. However, it will be assumed that the value of the integrals may be approximated by a weighted average of the values of the integrands at the planes $z = z_3$ and $z = z_4$. This is a strenuous approximation since it completely neglects the flow process between these planes. However, the weights are determined from solutions of the equations in each streamtube when the surface integrals are known at the measuring plane between the rotor trailing edge and the downstream measuring plane. The method of determining the weights will be discussed in Section 2.8.

Under this assumption and the assumption of axial symmetry, the quantities $R'_1$, $R'_2$, $R'_3$, and $R'_4$ may be rewritten in the following form:

$$R'_1 = \frac{2\Omega (z_4 - z_3)}{\sqrt{\kappa R}} \left\{ \frac{1 - W_1}{\sqrt{T'_3}} \int_{r31}^{r30} p_3 M'_3 \cos \gamma_3 \sin \beta_3 \left(1 + \frac{\kappa - 1}{2} M'^2_3\right)\left(1 - \frac{n\,th}{2\pi r}\right) dr + \frac{W_1 X'}{\sqrt{T'_4}} \right\} \tag{50}$$

where $X'$ is the integral evaluated at $z = z_4$

$$X' \equiv \int_{r40}^{r41} p_4 M'_4 \cos \gamma_4 \sin \beta_4 \left(1 + \frac{\kappa - 1}{2} M'^2_4\right)^{1/2} dr \tag{51}$$

and where $W_1$ is the weight associated with $X'$.

$$R'_2 = \frac{\Omega^2 (z_3 - z_4)}{\kappa R} \left\{ \frac{1 - W_2}{T'_3} \int_{r31}^{r30} p_3 \left(1 + \frac{\kappa - 1}{2} M'^2_3\right)\left(1 - \frac{n\,th}{2\pi r}\right)^2 dr + \frac{W_2 Y'}{T'_4} \right\} \tag{52}$$

where $Y'$ is the integral evaluated at $z = z_4$

$$Y' \equiv \int_{r_{4I}}^{r_{4O}} p_4 \left(1 + \frac{\kappa - 1}{2} M_4'^3\right) r^2 dr \tag{53}$$

and where $W_2$ is the weight associated with $Y'$.

$$R_3' = \frac{2\Omega (z_3 - z_4)}{\sqrt{\kappa R}} \left\{ \frac{1 - W_3}{\sqrt{T_3'}} \int_{r_{3I}}^{r_{3O}} p_3 M_3' \sin \gamma_3 \left(1 + \frac{\kappa - 1}{2} M_3'^2\right)^{1/2} \left(1 - \frac{n\,th}{2\pi r}\right) dr + \frac{W_3 Z'}{\sqrt{T_4'}} \right\} \tag{54}$$

where $Z'$ is the integral evaluated at $z = z_4$

$$Z' \equiv \int_{r_{4I}}^{r_{4O}} p_4 M_4' \sin \gamma_4 \left(1 + \frac{\kappa - 1}{2} M_4'^2\right)^{1/2} dr \tag{55}$$

and where $W_3$ is the weight associated with $Z'$.

$$R_4' = \frac{2\Omega (z_3 - z_4)}{\sqrt{\kappa R}} \left\{ \frac{1 - W_4}{\sqrt{T_3'}} \int_{r_{3I}}^{r_{3O}} p_3 M_3' \sin \gamma_3 \left(1 - \frac{\kappa - 1}{2} M_3'^2\right)^{1/2} \left(1 - \frac{n\,th}{2\pi r}\right) r^2 dr + \frac{W_4 Z''}{\sqrt{T_4'}} \right\} \tag{56}$$

where $Z''$ is the integral evaluated at $z = z_4$

$$Z'' \equiv \int_{r_{4I}}^{r_{4O}} p_4 M_4' \sin \gamma_4 \left(1 + \frac{\kappa - 1}{2} M_4'^2\right)^{1/2} r^2 dr \tag{57}$$

and where $W_4$ is the weight associated with $Z''$.

#### 2.5.4 Assumption 4

The quantity $F'$ of Eq. (30) could be calculated by an iteration process. According to Eq. (2), $p_3'$ is dependent on the axial Mach number, the area ratio, the free-stream static pressure, and the ratio of specific heats. Initially, it is assumed that $p_3'$ and the free-stream static pressure ($p_3$) are equal. Solution of the equations under this assumption yields the information for the evaluation of $p_3'$ by Eq. (2). This is then used to calculate $F'$, and solution of the equations is again obtained. The value of $p_3'$ is then recalculated according to Eq. (2) and the process continues until the values of $p_3'$ for two successive solutions differ

by less than some convergence criteria. To adapt this procedure, Eq. (27) is better written in the following form:

$$\int_{r_{3I}}^{r_{30}} p_3 \left[ M_3'^2 \cos^2 \gamma_3 \cos^2 \beta_3 \left( 1 - \frac{n\ th}{2\pi r} \right) + \frac{1}{\kappa} \right] r dr - K \frac{1}{\kappa} \frac{n}{2\pi} \int_{r_{3I}}^{r_{30}} p_3\ th\ dr$$

$$= D' + E' - K \frac{1}{\kappa} \frac{n}{2\pi} \int_{r_{3I}}^{r_{30}} p_3'\ th\ dr \tag{27'}$$

where for the initial solution K = 0.0 to indicate the terms involving $p_3$ and $p_3'$ cancel and for each successive solution K = 1.0. The results presented in this report are derived for K ≡ 0.0.

By using Eq. (40) for B', Eq. (46) for E', Eq. (50) for $R'_1$, Eq. (52) for $R'_2$, Eq. (54) for $R'_3$, and Eq. (56) for $R'_4$, it is possible to rewrite Eqs. (19), (24), (27), and (33) into a form for which the right hand side is independent of any unknown parameters at plane $z = z_3$.

$$\int_{r_{3I}}^{r_{30}} p_3 M_3'^2 \sin \gamma_3 \cos \gamma_3 \cos \beta_3 \left( 1 - \frac{n\ th}{2\pi r} \right) r dr + 2(r_{3I} r_{4I} - r_{30} r_{40})\, B_3'$$

$$- (r_{3I} - r_{30})\, B_4' + (r_{3I}^2 - r_{30}^2)\, B_5'$$

$$+ \frac{2\Omega(z_3 - z_4)}{\sqrt{\kappa R T_3'}} (1 - W_1) \int_{r_{3I}}^{r_{30}} p_3 M_3' \cos \gamma_3 \sin \beta_3 \left( 1 + \frac{\kappa - 1}{2} M_3'^2 \right)^{1/2} \left( 1 - \frac{n\ th}{2\pi r} \right) r dr$$

$$+ \frac{\Omega^2 (z_4 - z_3)}{\kappa R T_3'} (1 - W_2) \int_{r_{3I}}^{r_{30}} p_3 \left( 1 + \frac{\kappa - 1}{2} M_3'^2 \right) \left( 1 - \frac{n\ th}{2\pi r} \right) r^2 dr$$

$$= A' + (r_{40} - r_{4I})\, B_1' + (r_{40}^2 - r_{4I}^2)\, B_2' + \frac{2\Omega(z_4 - z_3)}{\sqrt{\kappa R T_4'}} W_1 X' + \frac{\Omega^2 (z_3 - z_4)}{\kappa R T_4'} W_2 Y' \tag{19'}$$

$$\int_{r_{3I}}^{r_{30}} p_3 M_3'^2 \cos^2 \gamma_3 \sin \beta_3 \cos \beta_3 \left( 1 - \frac{n\ th}{2\pi r} \right) r dr$$

$$+ \frac{2\Omega(z_4 - z_3)}{\sqrt{\kappa R T_3'}} (1 - W_3) \int_{r_{3I}}^{r_{30}} p_3 M_3' \sin \gamma_3 \left( 1 + \frac{\kappa - 1}{2} M_3'^2 \right)^{1/2} \left( 1 - \frac{n\ th}{2\pi r} \right) r dr$$

$$= C' + \frac{2\Omega(z_3 - z_4)}{\sqrt{\kappa R T_4'}} W_3 Z' \tag{24'}$$

$$\int_{r_{3I}}^{r_{30}} p_3 \left[ M_3'^2 \cos^2 \gamma_3 \cos^2 \beta_3 \left( 1 - \frac{n\ th}{2\pi r} \right) + \frac{1}{\kappa} \right] r dr + (r_{3I}^3 - r_{30}^3) \frac{B_5'}{z_4 - z_3} + (r_{3I}^2 - r_{30}^2) \frac{B_4'}{z_4 - z_3}$$

$$+ (r_{3I}^2 r_{4I} - r_{30}^2 r_{40}) \frac{E_1'}{z_4 - z_3} + (r_{3I} r_{4I}^2 - r_{30} r_{40}^2) \frac{E_2'}{z_4 - z_3} + (r_{3I} r_{4I} - r_{30} r_{40}) \frac{E_3'}{z_4 - z_3}$$

$$- K \frac{1}{\kappa} \frac{n}{2\pi} \int_{r_{3I}}^{r_{30}} p_3\ th\ dr = D' + (r_{4I}^3 - r_{40}^3) \frac{B_2'}{z_4 - z_3}$$

$$+ (r_{4I}^2 - r_{40}^2) \frac{B_1'}{z_4 - z_3} - K \frac{1}{\kappa} \frac{n}{2\pi} \int_{r_{3I}}^{r_{30}} p_3'\ th\ dr \qquad (27'')$$

$$\int_{r_{3I}}^{r_{30}} p_3 M_3'^2 \cos^2 \gamma_3 \sin \beta_3 \cos \beta_3 \left( 1 - \frac{n\ th}{2\pi r} \right) r^2 dr$$

$$- \frac{2\Omega(z_4 - z_3)}{\sqrt{\kappa R T_3'}} (1 - W_4) \int_{r_{3I}}^{r_{30}} p_3 M_3' \sin \gamma_3 \left( 1 + \frac{\kappa - 1}{2} M_3'^2 \right)^{1/2} \left( 1 - \frac{n\ th}{2\pi r} \right) r^2 dr$$

$$= H' + \frac{2\Omega(z_3 - z_4)}{\sqrt{\kappa R T_4'}} W_4 Z'' \qquad (33')$$

Note in Eq. (27'') that, although $p_3'$ is not actually a known quantity, the iteration procedure described previously would ensure a value of $p_3'$ for each iteration step.

Equations (19'), (24'), (27''), (31), and (33') represent the final form of the five equations describing the sudden area expansion process. The following section will describe the particular assumptions necessary to limit the unknowns on the left hand side to five.

## 2.6 ASSUMPTIONS CONCERNING THE PARTICULAR FUNCTIONAL FORM OF THE FLOW VARIABLES

### 2.6.1 Assumption 1

It has been assumed that static pressure varies linearly with radius across the annulus in order to evaluate integrals of streamtube boundary pressure forces. The flow variables are to be considered linear functions of radius in each streamtube so that radial changes from streamtube to streamtube may be represented by a continuous, piecewise-linear curve. These two approximations are consistent only if the static

pressure ($p_3$) is assumed linear across the annulus and not piecewise-linear; therefore, at $z = z_3$ the static pressure at any radius is determined from

$$p_3 = C_1 + C_2 r, \qquad r_h(z_3) \leq r \leq r_t(z_3) \tag{58}$$

where

$$C_2 = \frac{p_t(z_3) - p_h(z_3)}{r_t(z_3) - r_h(z_3)}$$

and

$$C_1 = p_t(z_3) - C_2 r_t(z_3)$$

The wall static pressure is measured at the tip, and, in order to specify the variation, it must be determined at one other point, such as the hub wall. Such a value has been extrapolated from other measurements on the hub wall to evaluate the integrals of the resultant force due to pressure on the stream surfaces, and this pressure must be used to yield the necessary function in the solutions here. However, this is a very strenuous assumption since the extrapolated pressure does not necessarily obey any of the laws of fluid flow. The extrapolation is felt to yield reasonable but, certainly, unjustifiable estimates of the hub wall static pressure at the plane of the rotor trailing edge.

By considering the simplification that this approximation provides in allowing direct integration of $B'_i$, $i = 1, 2, \ldots, 5$, and $E'_1$, $i = 1, 2, 3$, considering the limited number of equations available to determine the flow variables at $z = z_3$, and considering the other simplifications necessary to this problem, then the extrapolation to obtain $p_h(z_3)$ is justified; but it is noted that improvement in this assumption should be considered necessary in a more advanced solution of this problem.

#### 2.6.2 Assumption 2

The relative flow angle at the blade trailing edge ($\beta_3$) is assumed to vary linearly in each streamtube; i. e.,

$$\beta_3 = b_1 + b_2 r, \qquad r_{31} \leq r \leq r_{30} \tag{59}$$

Use of the integral equations that are being applied to the sudden expansion flow process demands that there exist no flow separation at either the entrance to or the exit from the bounded flow region between $z_3$ and $z_4$. Therefore, this demand is obeyed if the solution for $\beta_3$ deviates very little from the average angle of the blade trailing edge ($\beta_3'$).

Furthermore, cascade tests have shown that $\beta_3$ is greater than $\beta_3'$ except in end wall regions where secondary flows may cause $\beta_3$ to be less than $\beta_3'$. These considerations are expected to form one basis for judging the applicability of the present method for solution of the sudden expansion flow process.

#### 2.6.3 Assumption 3

The sine of the relative pitch angle ($\gamma_3$) is assumed to vary linearly in each streamtube; i. e.,

$$\sin \gamma_3 = g_1 + g_2 r, \qquad r_{31} \leq r \leq r_{30} \tag{60}$$

From the assumption in derivation that flow may only enter the region at $z = z_3$, the value of $\sin \gamma_3$ is limited to values between +1 and -1; i.e., $-90° \leqslant \gamma_3 \leqslant +90°$.

#### 2.6.4 Assumption 4

The relative Mach number ($M'_3$) is assumed to vary linearly within each streamtube; i. e.,

$$M'_3 = d_1 + d_2 r, \qquad r_{31} \leq r \leq r_{30} \tag{61}$$

#### 2.6.5 Assumption 5

The thickness-to-radius ratio (th/r) may be considered the angular distance per blade at a fixed radius through which no flow may enter the control volume. In real flows, this angular distance would be composed of the angle subtended by both the blade trailing edge and some flow defect that is due to boundary layer accumulation on the blades. However, the governing equations are frictionless and axisymmetric and contain no mechanism that would determine this angular distance. The equations certainly do prescribe a certain flow area, but they give no preference as to its linear dimensions, whether tangential or radial. This implies that either th/r or the stream surface locations at the blade trailing-edge plane must be specified. In the present solution, th/r is specified as the blade trailing-edge thickness-to-radius ratio, while the stream surface locations are demanded from the solution.

Since a certain flow area is required by the equations and since the measurements used to calculate various terms in the equations are results of real flows, it is reasonable to expect that some flow defect will show up in the overall calculations. For instance, the flow area may not extend radially from the hub completely to the tip. This yields a

flow area defect, or blockage, which is theoretically due to the frictional effects that are ignored in the problem but may also include measurement errors. Examples of the frictional effects include the boundary layer blockage at the trailing edge, annulus wall friction, and the friction at the planes of entrance to and exit from the control volume. The flow defect is a result of all these factors, and each component is indistinguishable from the other. Therefore, the blockage factor is characteristic of the friction in the general flow process and not necessarily representative of the actual boundary layer blockage at the trailing edge.

From consideration of Eqs. (19′), (24′), (27″), (31), and (33′) and Eqs. (59), (60), and (61) describing the functional form of the variables, the following quantities must be specified by solution of the equations in each streamtube: $r_{3I}$, $r_{3O}$, $b_1$, $b_2$, $g_1$, $g_2$, $d_1$, $d_2$. Since there are five equations, only five of these quantities can be determined. The following section outlines the selection of the proper five constants to be determined and the method of solution.

## 2.7 SELECTION OF UNKNOWNS AND METHOD OF SOLUTION

Substitution of Eq. (61) into Eq. (27″) leads to the following quadratic formulation of Eq. (27″) in terms of $d_1$:

$$d_1^2 V_1 + 2d_1 d_2 V_2 + d_2^2 V_3 - \text{RHS}(27'') = 0 \tag{62}$$

where

$$\text{RHS}(27'') = D' + (r_{4I}^3 - r_{40}^3)\frac{B_2'}{z_4 - z_3} + (r_{4I}^2 - r_{40}^2)\frac{B_1'}{z_4 - z_3}$$

$$- k\frac{1}{\kappa}\frac{n}{2\pi}\left[\int_{r_{3I}}^{r_{3O}} p_3' \, {}^{th}\, dr - \int_{r_{3I}}^{r_{3O}} p_3 \, {}^{th}\, dr\right] - \frac{1}{\kappa}\int_{r_{3I}}^{r_{3O}} p_3 \, r dr$$

$$- (r_{3I}^3 - r_{3O}^3)\frac{B_5'}{z_4 - z_3} - (r_{3I}^2 - r_{3O}^2)\frac{B_4'}{z_4 - z_3} - (r_{3I}^2 r_{4I} - r_{3O}^2 r_{4O})\frac{E_1'}{z_4 - z_3}$$

$$- (r_{3I} r_{4I}^2 - r_{3O} r_{4O}^2)\frac{E_2'}{z_4 - z_3} - (r_{3I} r_{4I} - r_{3O} r_{4O})\frac{E_3'}{z_4 - z_3}$$

and where

$$[V_1, V_2, V_3] = \int_{r_{3I}}^{r_{3O}} p_3 \cos^2 \gamma_3 \cos^2 \beta_3 \left(1 - \frac{n \, th}{2\pi r}\right) [r, r^2, r^3] \, dr$$

The rearrangement of Eq. (27'') into Eq. (62) is very important because, as will be shown, it eliminates the necessity of iteration on one of the five equations since $d_1$ can be determined exactly, satisfying Eq. (62), if the other variables are known or guessed.

To begin the solution, the particular streamtube is selected for which the overall relative total pressure loss was a minimum. The variables, $\beta_3$, $\sin\gamma_3$, and $M_3'$, are assumed constant over the entire radial height of this initial streamtube, i. e., $b_2 = g_2 = d_2 = 0$. Thus, for the initial streamtube, $d_1$ may be determined from

$$d_1 = + [\text{RHS}(27'')/V_1]^{1/2} \tag{62'}$$

and there remains exactly five undetermined constants, $r_{30}$, $r_{31}$, $b_1$, $g_1$, $d_1$, to be found by solution of the five governing equations, Eqs. (19'), (24'), (63'), (31), and (33'). The iteration process leading to solution is illustrated in Fig. 7, and the convergence criterion guarantees at least six significant digits for each variable.

The solution of the initial streamtube provides boundaries of that streamtube and the values which $\beta_3$, $\sin\gamma_3$, and $M_3'$ must have at these boundaries in the neighboring streamtubes. It is demanded that the solution values be continuous across the common boundary between two streamtubes. Then, the following conditions must be satisfied for every streamtube except the initial one:

$$b_2 = (\beta_B - b_1)/r_B \tag{63}$$

$$g_2 = (\sin\gamma_B - g_1)/r_B \tag{64}$$

$$d_2 = (M'_B - d_1)/r_B \tag{65}$$

where $r_B$, $\beta_B$, $\sin\gamma_B$, and $M'_B$ are determined from the solution in a neighboring streamtube. Since one of the streamtube bounding radii is determined from the solution of a neighboring streamtube, the number of unknown quantities has been reduced from eight to seven. The three additional relations, Eqs. (63), (64), and (65), give a total of eight equations so that the problem is not solvable unless one of the five governing equations is dropped. The axial component of the moment of momentum, Eq. (33'), was eliminated since it really supplies no more information to the system of equations than the tangential component of the momentum equation, Eq. (24').

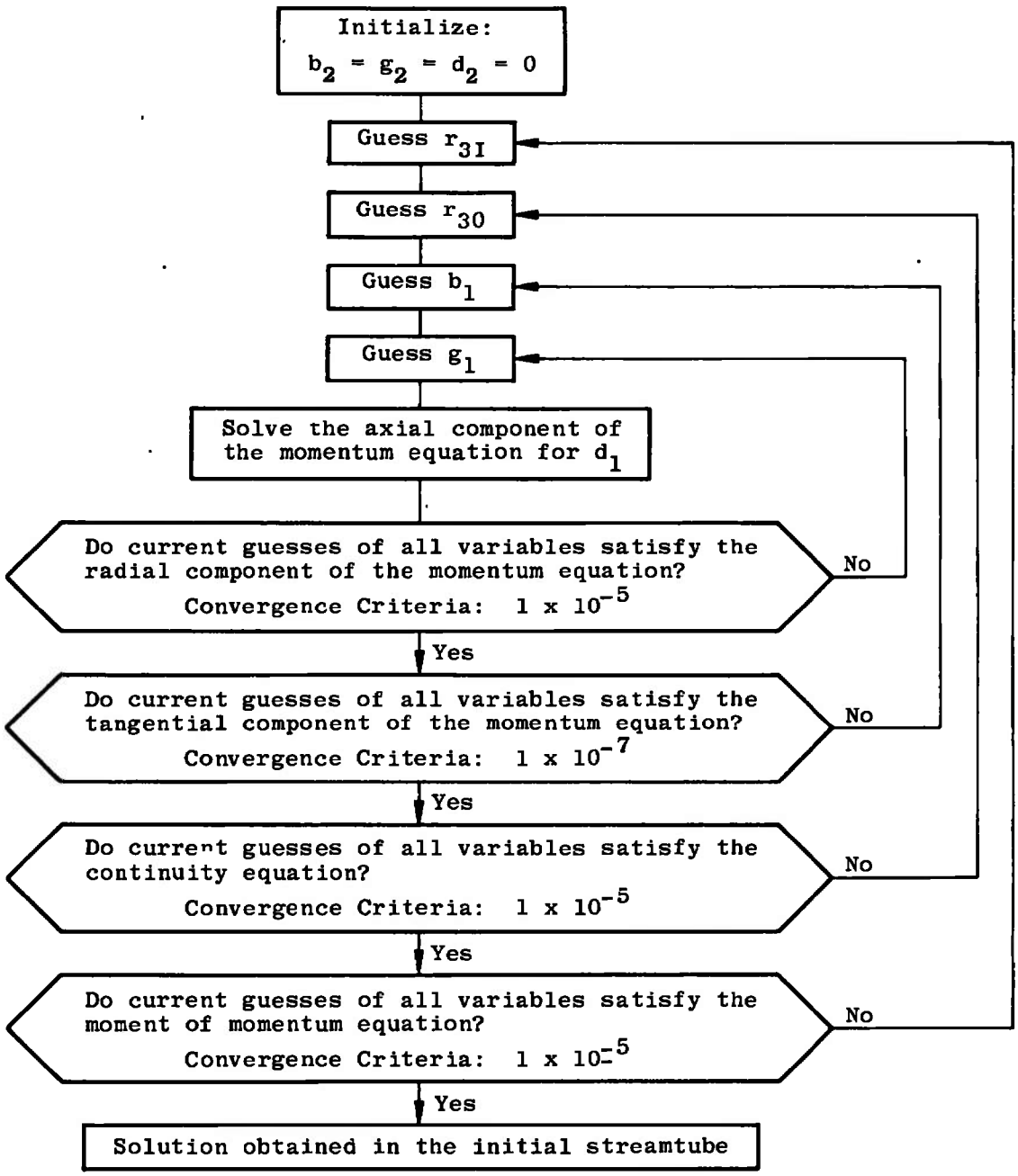


Fig. 7 Iteration Scheme for the Initial Streamtube

If Eq. (65) is substituted into Eq. (62), the following relation results:

$$A\,d_1^2 + B\,d_1 + C = 0$$

where

$$A = V_1 - 2\frac{V_2}{r_B} + \frac{V_3}{r_B^2}$$

$$B = 2M_B'\left[\frac{V_2}{r_B} - \frac{V_3}{r_B^2}\right]$$

$$C = M_B'^2\frac{V_3}{r_B^2} - \mathrm{RHS}(27'')$$

with the solution

$$d_1 = \frac{-B \pm \sqrt{B^2 - 4AC}}{2A} \qquad (62'')$$

Experience has shown that, in general, the positive sign on the radical is applicable when the upper boundary of the streamtube is known and the negative sign applies when the lower boundary is known.

The iteration cycle yielding solution of Eqs. (19′), (24′), (62″), and (31) is illustrated in Fig. 8. The convergence factors guarantee at least six significant figures for each variable.

It remains to comment here that, even though the scheme is straightforward, simple, and relatively certain of finding a solution if it exists, the method is time consuming. One complete case takes approximately 15 min of computation time for the IBM 360/50 computer in accomplishing 7000 or more iteration steps to obtain reasonable accuracy. Therefore, a much faster scheme must be sought if the problem is to be economically solved. The present iteration scheme serves only to demonstrate that the problem can be solved and to acquire a few example results.

## 2.8 DETERMINATION OF THE WEIGHTS FOR EVALUATION OF THE VOLUME INTEGRALS

Obtaining and correlating values for the weights $W_i$ ($i = 1, 2, 3, 4$) in Eqs. (50), (52), (54), and (56) presents a formidable problem in itself. In essence, the task is to find values of $W_i$ which, when substituted into Eqs. (50), (52), (54), and (56), give good approximations of the values of $R'_1$, $R'_2$, $R'_3$, and $R'_4$ obtained by more accurate evaluations of Eqs. (22), (23), (26), and (35). These evaluations may involve

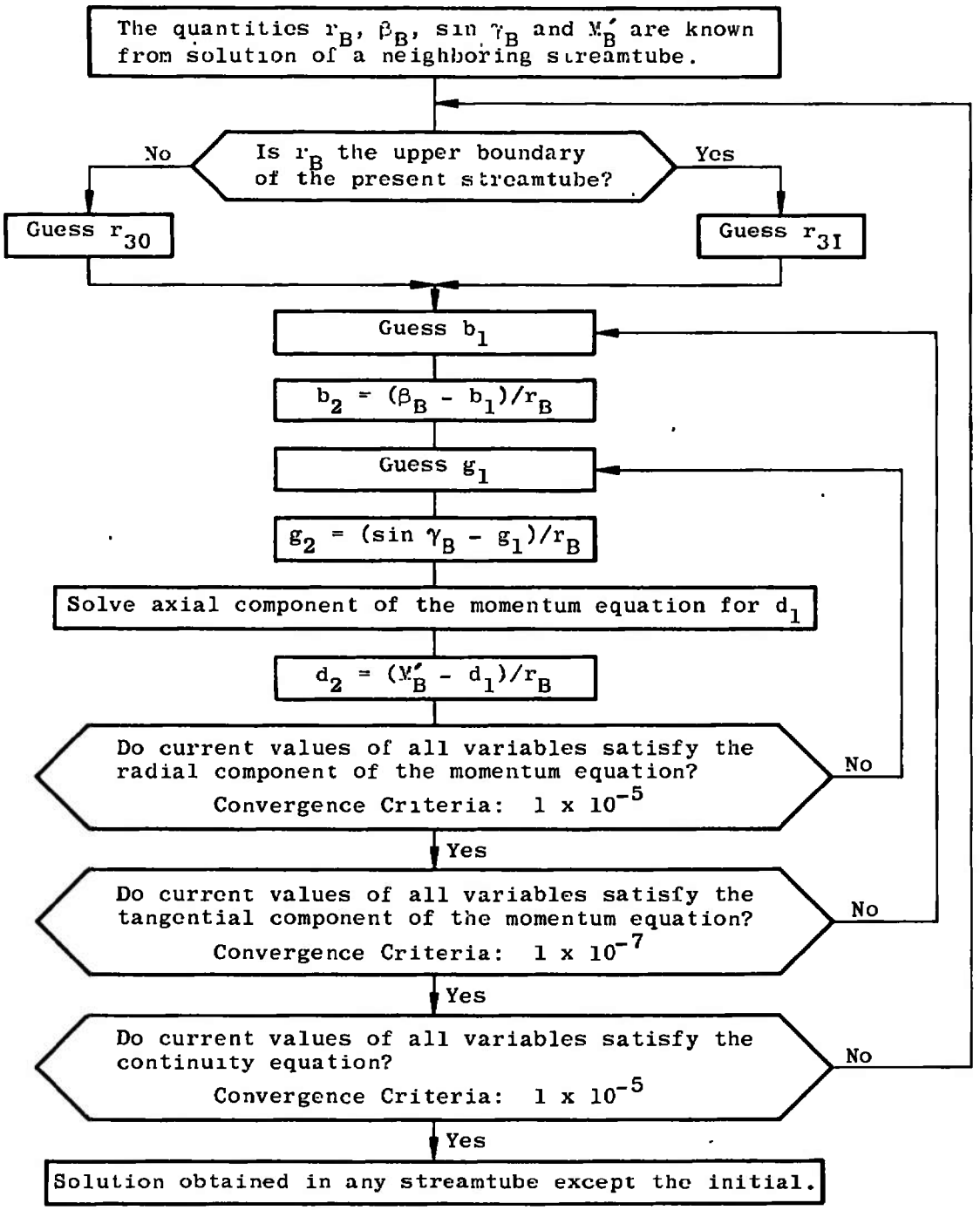


Fig. 8 Iteration Scheme for Solution of All Streamtubes except the Initial Streamtube

measurements at other planes z, $z_3 < z < z_4$. However, in fluctuating flow fields, such as those experienced behind a rotor, measurement interpretation becomes questionable. Therefore, even the more accurate evaluations of the volume integrals probably only represent low order approximations.

With this in mind consider the following simple approach. For the particular case under consideration, measurements of the flow properties are available 2 in. downstream of the rotor trailing edge. This is interpreted as the plane $z = z_4$. In a few cases, measurements are simultaneously taken at a distance of 1/2 in. behind the rotor. This plane will be specified $z = z_e$. Assuming a straight-line variation of the integrals between the z stations allows the approximation of the volume integrals in the following manner for axisymmetric flow:

$$R'_A = \frac{\Omega}{\sqrt{\kappa R}} \left\{ \frac{z_e - z_3}{\sqrt{T'_3}} \int_{r_{3I}}^{r_{3O}} p_3 M'_3 \cos\gamma_3 \sin\beta_3 \left(1 + \frac{\kappa - 1}{2} M'^2_3\right)^{\frac{1}{2}} \left(1 - \frac{n\,th}{2\pi r}\right) dr \right.$$

$$\left. + \frac{1}{\sqrt{T'}} \left[ \cos\gamma_e \frac{A_e}{A_{e_{geo}}} X'_e (z_4 - z_3) + X'(z_4 - z_e) \right] \right\} \tag{66}$$

where

$$X'_e \equiv \int_{r_{eI}}^{r_{eO}} p_e M'_e \sin\beta_e \left(1 + \frac{\kappa - 1}{2} M'^2_e\right)^{\frac{1}{2}} dr \tag{67}$$

and where $X'$ is given by Eq. (51)

$$R'_{2A} = \frac{\Omega^2}{2\kappa R} \left\{ \frac{z_e - z_e}{T'_3} \int_{r_{3I}}^{r_{3O}} p_3 \left(1 - \frac{\kappa - 1}{2} M'^2_3\right) \left(1 - \frac{n\,th}{2\pi r}\right) r^2 dr \right.$$

$$\left. + \frac{1}{T'} \left[ \frac{A_e}{A_{e_{geo}}} Y'_e (z_3 - z_4) + Y'(z_e - z_4) \right] \right\} \tag{68}$$

where

$$Y'_e \equiv \int_{r_{eI}}^{r_{eO}} p_e \left(1 + \frac{\kappa - 1}{2} M'^2_e\right) r^2 dr \tag{69}$$

and where $Y'$ is given by Eq. (53)

$$R'_{3A} = \frac{\Omega}{\sqrt{\kappa R}} \left\{ \frac{z_3 - z_e}{\sqrt{T'_3}} \int_{r_{3I}}^{r_{3O}} p_3 M'_3 \sin\gamma_3 \left(1 + \frac{\kappa - 1}{2} M'^2_3\right)^{\frac{1}{2}} \left(1 - \frac{n\,th}{2\pi r}\right) dr \right.$$

$$\left. + \frac{1}{\sqrt{T'}} \left[ \sin\gamma_e \frac{A_e}{A_{e_{geo}}} Z'_e (z_3 - z_4) + Z'(z_e - z_4) \right] \right\} \tag{70}$$

where

$$Z'_e \equiv \int_{r_{el}}^{r_{e0}} \rho_e M'_e \left(1 + \frac{\kappa - 1}{2} M_e'^2\right)^{\frac{1}{2}} r dr \tag{71}$$

and where $Z'$ is given by Eq. (55)

$$R'_{iA} = \frac{\Omega}{\sqrt{\kappa R}} \left\{ \frac{z_3 - z_e}{\sqrt{T'_3}} \int_{r_{31}}^{r_{30}} \rho_3 M'_3 \sin \gamma_3 \left(1 + \frac{\kappa - 1}{2} M'^2_3\right)^{\frac{1}{2}} \left(1 - \frac{n\,th}{2\pi r}\right) r^2 dr \right.$$

$$\left. - \frac{1}{\sqrt{T'}} \left[ \sin \gamma_e \frac{A_e}{A_{e_{geo}}} Z''_e (z_3 - z_4) + Z'' (z_e - z_4) \right] \right\} \tag{72}$$

where

$$Z''_e = \int_{r_{el}}^{r_{e0}} \rho_e M'_e \left(1 - \frac{\kappa - 1}{2} M'^2_e\right)^{\frac{1}{2}} r^2 dr \tag{73}$$

and where $Z''$ is given by Eq. (57). In each case $T'$ represents an average of $T'_e$ and $T'_4$ which should partially account for heat transfer.

A certain inaccuracy is admitted in these equations over and above the measurement uncertainty. This report considers tests for which the pitch angle has not been measured. If the plane $z = z_4$ is sufficiently far downstream, it is expected that the direction of the flow would be in the average direction of the bounding walls. For the case of cylindrical bounding walls, $\gamma_4 = 0$, however, at the plane $z = z_e$, such an approximation may not be realistic. Instead, the pitch angle ($\gamma_e$) is assumed constant, hence its removal from the integrals of $X'_e$ in Eq. (66), $Z'_e$ in Eq. (70), and $Z''_e$ in Eq. (72), and it is to be related to the average direction of the streamtube walls at the plane $z = z_e$.

By using Fig. 6, the following relations may be derived:

$$M'_{ez} = M'_e \cos \gamma_e \cos \beta_e$$

$$\tan \gamma_{ez} = \frac{M'_{er}}{M'_{ez}}$$

$$\sin \gamma_e = \frac{M'_{er}}{M'_e}$$

where $\gamma_e$ is the angle between $M'_e$ and the projection of $M'_e$ into a tangential plane and where $\gamma_{ez}$ is the angle between $M'_{ez}$ and the projection of $M'_e$ into a radial plane. These relations lead to

$$\tan \gamma_e = \tan \gamma_{ez} \cos \beta_e$$

$$\sin \gamma_c = \frac{\tan \gamma_{cz} \cos \beta_e}{\sqrt{1 + \tan^2 \gamma_{ez} \cos^2 \beta_e}}$$

$$\cos \gamma_e = \frac{1}{\sqrt{1 + \tan^2 \gamma_{ez} \cos^2 \beta_e}}$$

For the purposes of this approximation, $\beta_e$ in these relations is taken as the mass-averaged relative flow angle in each streamtube, and $\gamma_{ez}$ is given by

$$\tan \gamma_{ez} = \frac{1}{4}\left[\frac{r_{e0} - r_{30}}{z_e - z_0} + \frac{r_{e1} - r_{31}}{z_e - z_0} + \frac{r_{40} - r_{e0}}{z_4 - z_e} + \frac{r_{41} - r_{e1}}{z_4 - z_e}\right]$$

Unfortunately, the addition of the estimated value of $\gamma_e$ results in only about 1-percent correction of the continuity balance so that the remaining error may be due to inaccuracies in flow property measurements. It is now the problem to force the continuity equation to balance through the planes $z_e$ and $z_4$, but it is not feasible to apply theoretical correction factors to each of the flow property measurements. Therefore, it is reasoned that the unsteady flow at the plane $z = z_e$ may be represented as the periodic passing of conditions of zero mass flow and the full mass flow per blade passage. The sum total of the mass flow per passage is set equal to the total mass flow measured at the plane $z = z_4$. This procedure will then yield a blockage factor $(A_e/A_{e_{geo}})$ to be applied to the integrals evaluated at $z = z_e$. Essentially, the assumption is that the blocked area of zero mass flow is so small in terms of time and the time constants for the sensors are so long that the effects of the zero mass flow sections is not noted in the measurements.

Certain errors may appear with the use of this correction factor. These are related to the fact that $\gamma$ has been ignored in the tests to date. Both the total mass flow and the radial locations of the stream surfaces at $z = z_e$ could be affected. The effect should be small since the mass flow depends on the cosine of this angle.

It is noted that the correction factor directly results from the continuity equation and that it is used on certain terms of momentum conservation equations. Although an analogous correction factor could be derived from the one-dimensional momentum equation, such a factor accounts for shear forces and may be highly sensitive to the shearing effects that naturally occur in this flow problem. The only real solution to this problem is the correction of every measurement to account for the very turbulent, unsteady flows that must occur. Such a task is beyond the scope of this report.

Since $R'_{1A}$ has been obtained by Eq. (66), it is a simple matter to set this value equal to Eq. (50) and then to solve for $W_1$. The weights $W_2$, $W_3$, and $W_4$ may be found in a similar manner. This process has guaranteed that the volume integrals are equal; however, it has not ensured the equality of the solutions by both methods. This fact is brought about by the new approximations of the terms $B'$ of Eq. (21) and $E'$ of Eq. (29) which have to be made since $r_{3O}$, $r_{eO}$, and $r_{4O}$, as well as $r_{3I}$, $r_{eI}$, and $r_{4I}$, may not be colinear points. However, since the difference between the static pressure on hub and tip walls is not very large, the differences in the solutions should be small. At any rate, it is timewise more advantageous to directly calculate the weights by equality of volume integrals rather than through an iteration process for the weights guaranteeing equality of solutions.

In general, it is unlikely that the representation of the volume integrals given by Eqs. (66), (68), (70), and (72) represent more than a first-order evaluation. Improvement of this scheme can come, first, through actual measurement of the pitch angles, and second, through providing more measurements at various planes between $z_3$ and $z_4$. Certainly, more elaborate representations of the volume integrals may be made with the available data. For instance, a quadradic approximation of the integrands may be hypothesized rather than the linear variation assumed here; however, the basic uncertainty in the interpretation of the measured data lends doubt that the more complex approximation would increase accuracy.

## SECTION III
## RESULTS OF CALCULATION

The following paragraphs present the calculation results for rotor R1C2 to exemplify some of the data which can be obtained from solution of the two-dimensional sudden area expansion flow process. The rotor is described in Ref. 2, and the measured data are summarized in that report. Because of the excessive computation time required, it was necessary to limit the investigation to one rotor and, in general, to the cases of maximum pressure ratio operating conditions for each speed line. These conditions are the most interesting because maximum efficiency generally occurs at these conditions for the rotors tested thus far. One speed line has been selected, however, for which calculations were performed for all operating conditions in order to examine the variation of sudden area expansion loss with absolute total pressure ratio. A description of the quasi-two-dimensional solution is provided in Appendix I for comparison purposes.

### 3.1 DETERMINATION OF THE WEIGHT NUMBERS

The weight numbers are determined such that, in each streamtube, the volume integrals calculated using a weighted average of the surface integrals at $z = z_3$ and $z = z_4$ are equivalent to the volume integrals calculated by assuming straight-line variation of the surface integrals with axial position between the rotor trailing-edge plane and the plane of extra measurements and between the plane of extra measurements and the downstream measuring plane. This procedure is possible only when the necessary extra flow property measurements are available; and, at present, this corresponds to the maximum-pressure-ratio operating conditions only.

Figure 9 is a plot of the calculated weight numbers in function of the radial position of the streamtube centers at the downstream measuring plane. Results have shown that $W_3$ and $W_4$ are very nearly equivalent. This could have been expected since both determine essentially the same parameter; i.e., the tangential component of the volume integral for the force due to Coriolis acceleration (see Eqs. (54) to (57)).

First-order dependence of the weight numbers on the proximity of the hub and tip walls is evident. This probably results from the influence of annulus wall friction on the measured data. It is noted that $W_3$ and $W_4$ are least influenced by wall proximity.

The weight numbers, especially $W_1$ and $W_2$, are noted to be widely scattered. They exhibit no apparent dependence on such parameters as wheel speed, Mach number at the downstream measuring station, etc. It was originally intended to correlate these weight numbers in order to attempt calculations at conditions for which the extra flow property measurements do not exist. The correlation could be valuable for calculations at maximum pressure ratio operating conditions when it is desired to interpolate between constant speed characteristics, but it may not be applicable to constant speed characteristics when the absolute total pressure ratio is not maximum. A correlation applicable to the latter case would be of more significance for this purpose, but it is not possible to guarantee the reliability of such a correlation using the data currently available. Therefore, the correlation has not been attempted.

It has been pointed out that there will probably exist a difference between the solutions obtained when the extra plane of measurements are used in calculating the volume integrals and when the weight numbers are used. These differences were suggested to be due mainly to

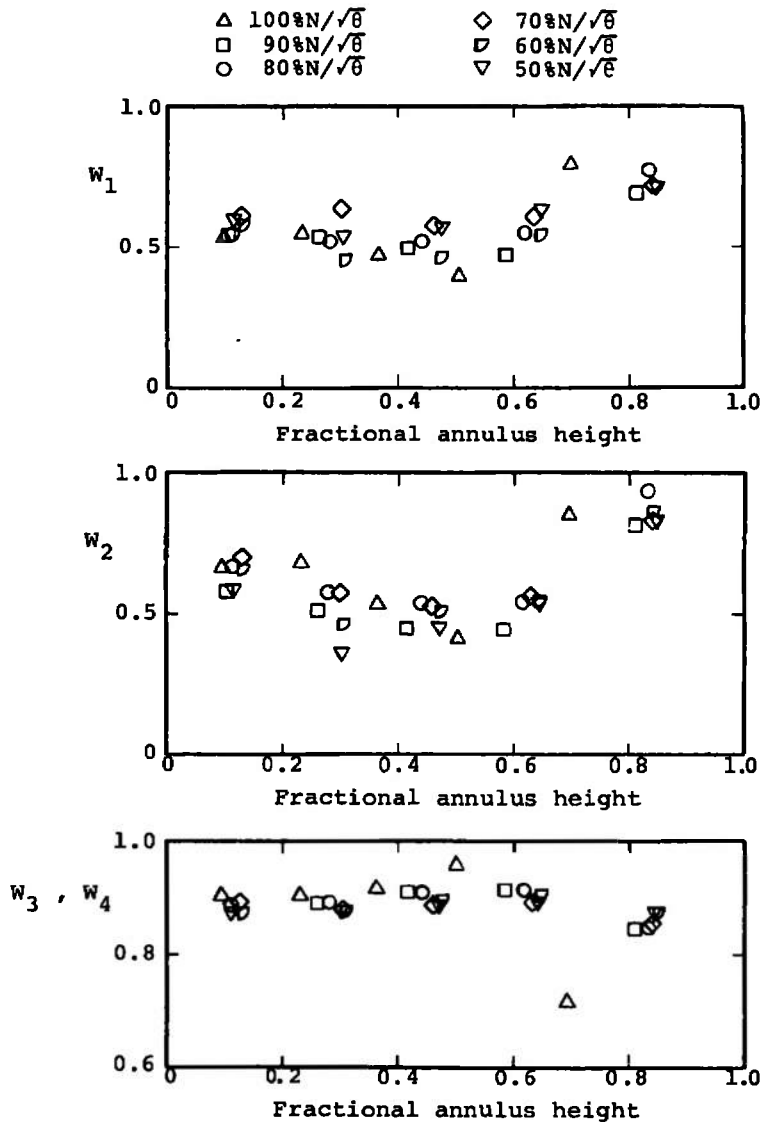


**Fig. 9 Variation of Weight Numbers as a Function of the Radial Position of the Streamtube Centers at the Downstream Measuring Plane**

differences in pressure-induced forces resulting from the two geometrical approximations of the streamtube bounding walls. Figure 10 compares the results of solution using the extra plane of measurements with the results using the calculated weight numbers for the 90-percent $N/\sqrt{\theta}$ data point. This plot is typical of such results, and it is noted that major differences in the two solutions occur in the streamtube nearest the tip where the geometrical differences in the streamtubes are the greatest. As the hub wall is approached, the solutions become more nearly the same.

In the presentation of the general results which follows, the results derived from the solution are examined using the weights rather than the solution determining the weights because only this alternative is available when the extra plane of measurements does not exist. It is apparent from Fig. 10 that this solution produces results that are less erratic in the streamtube nearest the tip.

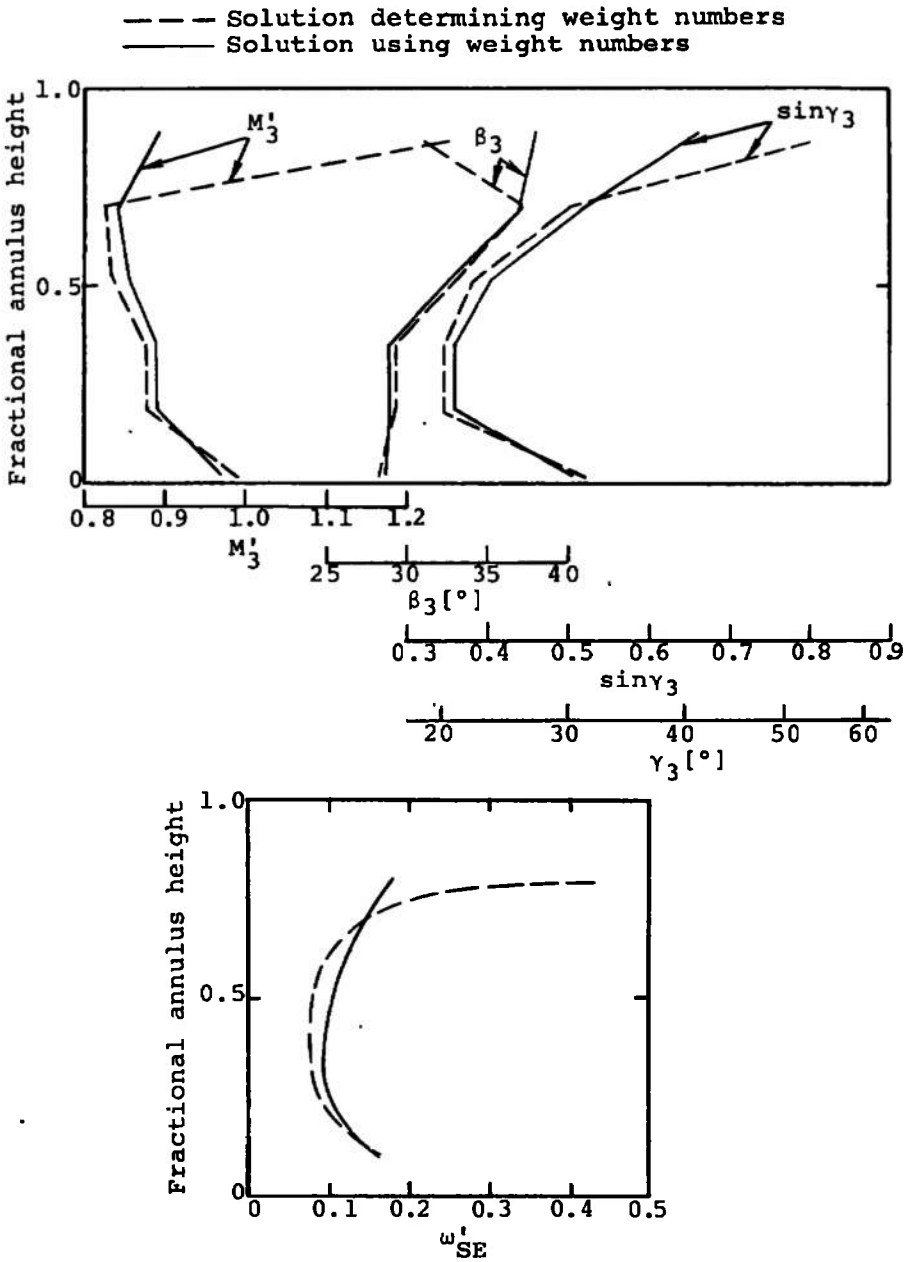


Fig. 10 Comporison of Solutions Determining Weight Numbers with Solutions Using Weight Numbers at 90-percent $N/\sqrt{\theta}$

### 3.2 GENERAL RESULTS OF THE TWO-DIMENSIONAL SOLUTION

Solution of the two-dimensional sudden area expansion problem yields the radial variation of the relative Mach number ($M_3'$), the relative yaw angle ($\beta_3$), and the relative pitch angle ($\gamma_3$) as well as an estimate of the stream surface radial locations at the trailing-edge plane. Figure 11 presents the radial variation of $M_3'$ and $\beta_3$, the deviation angle $\delta_3$ (i.e., the difference between $\beta_3$ and the blade angle at the trailing edge), and $\gamma_3$ for various rotational speeds of rotor R1C2 at maximum absolute total pressure ratio operating conditions. These results should represent circumferentially averaged values at each radial station in the trailing-edge plane. The relative Mach number is seen to decrease with decreasing rotational speed, and this is consistent with the decrease in the relative Mach number at the wheel inlet.

The relative yaw angle is more easily understood through its relation to the exit blade angle. The deviation angle ($\delta$) depicts such a representation, and it should be positive since conditions of overturning by blading are rarely observed in practice. Within the limitations of the problem concept, this practical condition is very nearly met at all rotational speeds except 100-percent $N/\sqrt{\theta}$. Evidently, the flow field at design speed is such that the basic assumptions of the problem are grossly violated.

The results for the relative pitch angle indicate that this angle increases with decreasing wheel speed. Such a result is extremely surprising since the radial forces in the wheel are not expected to be sufficiently high to justify this result. It will be shown in a later section that this discrepancy can be directly related to neglecting frictional effects.

The results for the radial shifting of streamtubes indicate, in general, that all streamtube centers, except the one nearest the tip, are located between their known positions upstream and downstream of the rotor, but at higher rotational speeds (70-percent $N/\sqrt{\theta}$ and above), most of the shift apparently occurs within the rotor. Again in reference to the higher speeds, it appears that the streamtube center nearest the rotor tip is even further depressed than is indicated by the streamtube center locations at the measuring plane 2.0 in. downstream of the rotor. The magnitude of the depression that must occur within the rotor decreases with wheel speed. These results can be directly related to the use of the extra plane of measurements located 0.5 in. downstream of the rotor, but they also infer that the difficulty in the flow field indicated by the wall static pressure measurements downstream of the rotor (see Refs. 2 or 9 or Fig. 26 of Ref. 8) probably results from separated flow within the rotor.

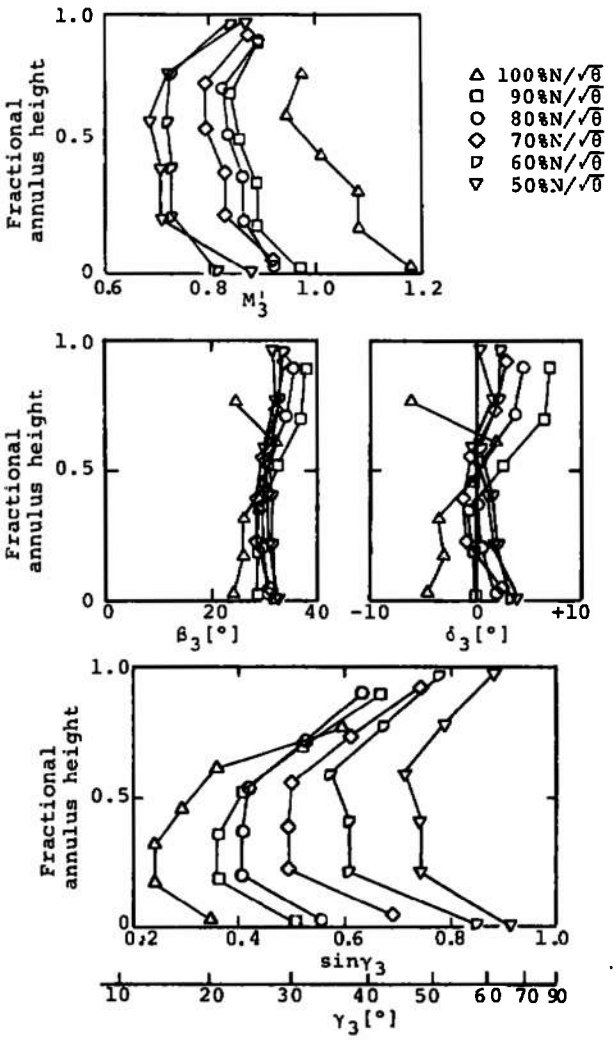


**Fig. 11 Solution Results for Rotor R1C2 for Various Rotor Speeds at Maximum Absolute Total Pressure Ratio Operating Conditions**

The main objective of these calculations has been the determination of the loss in relative total pressure attributable to the mixing process which occurs when the flow leaves the rotor blade passages. The calculated flow properties at the rotor trailing edge allow the estimation of an average relative total pressure in each streamtube, and this average value is used to calculate the loss by the equation:

$$\omega'_{SE} = \frac{P_3 - P_4}{P_2 - p_2}$$

The radial variation of sudden area expansion loss is shown in Fig. 12. There is a direct correspondence between $\omega'_{SE}$ in this figure and the solution for sin $\gamma_3$ shown in Fig. 11 demonstrating that $\omega'_{SE}$ is extremely

dependent on the radial component of the flow velocity. However, it is very doubtful that the radial component behaves as the present solutions indicate. This point will be examined in a later section.

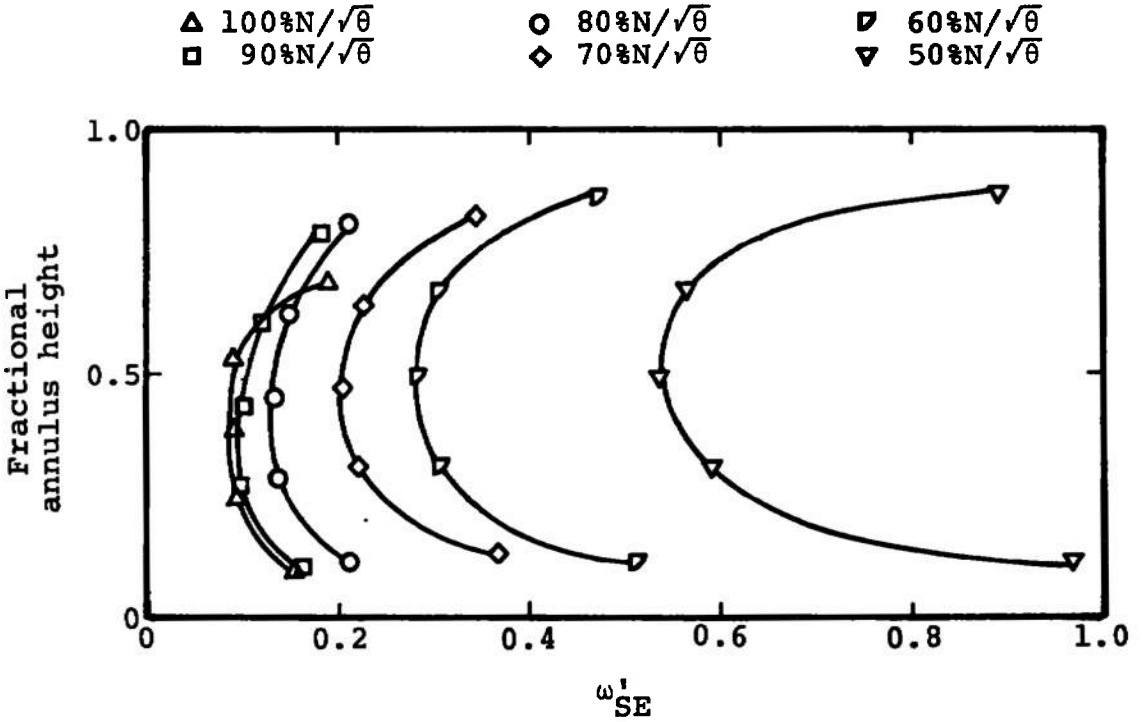


Fig. 12 Calculated Radial Variation of $\omega'_{SE}$ for Rotor R1C2 for Various Wheel Speeds at Maximum Absolute Total Pressure Ratio Operating Conditions

Figure 13 shows the variation of $\omega'_{SE}$ as a one-dimensional parameter for conditions of maximum absolute total pressure ratio in comparison to the variation of the overall relative total pressure loss. Three points are shown for each rotational speed. These indicate the repeatability of the measurements since the three points were taken at approximately the same operating conditions and emphasize the small effect of repeatability on the solutions.

The results shown in this figure indicate that $\omega'_{SE}$ is grossly overestimated in the lower speed range since $\omega'_{SE}$ cannot physically be greater than $\bar{\omega}'$. This fact and the direct relationship between $\omega'_{SE}$ and $\gamma_3$ tend to indicate that the solutions for $\gamma_3$ are physically unrealistic in the lower speed ranges.

It is, of course, uncertain that any of the two-dimensional solutions presented here are valid approximations to the real flow process. Since the overall relative total pressure loss is composed of sudden area

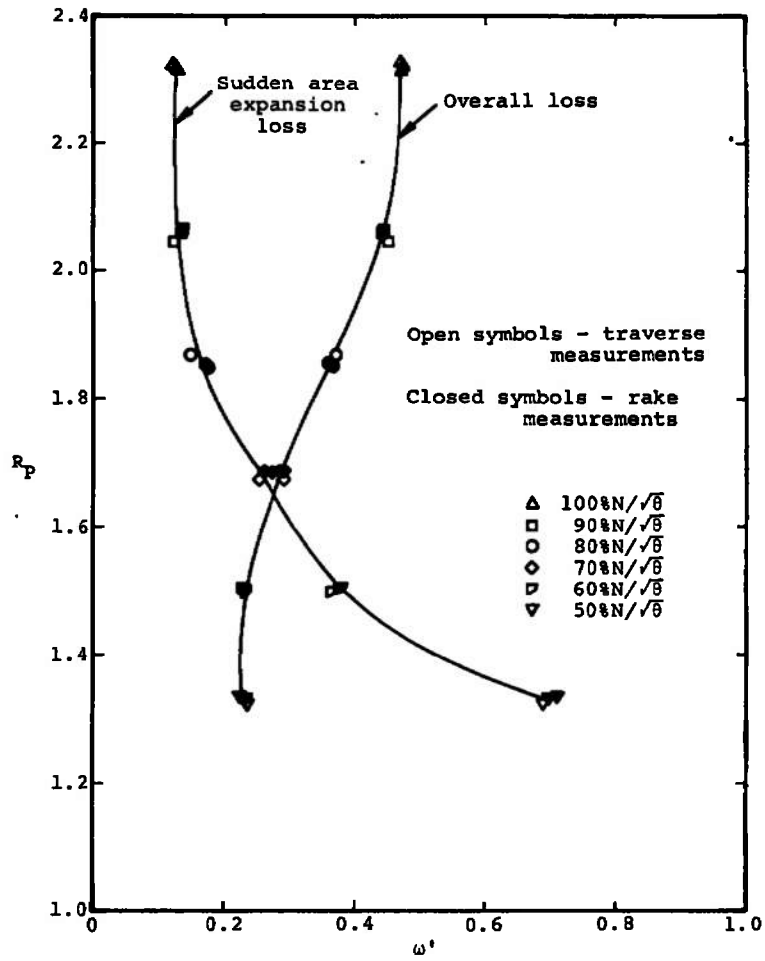


**Fig. 13 Comparison of the Annulus Average Relative Total Pressure Loss Coefficient due to Sudden Area Expansion with the Measured Overall Loss at Maximum Absolute Total Pressure Ratio Operating Conditions**

expansion loss, passage shock loss, and profile loss, it is certain that all solutions below 80-percent $N/\sqrt{\theta}$ are invalid because in these cases the sum of the calculated sudden area expansion loss and a reasonable estimate of the shock losses occuring within the blade passage is greater than the measured overall loss. Even the 80-percent $N/\sqrt{\theta}$ case is very close to violating this condition. However, in an effort to determine the influence of the absolute total pressure ratio for constant wheel speed operation, the solution for the 90-percent $N/\sqrt{\theta}$ speed line has been obtained. To perform the calculations, the weight numbers, determinable only at the maximum total pressure ratio, were assumed constant for the entire speed line. Example solution results are shown in Fig. 14, and the general behavior of the solutions appears quite reasonable.

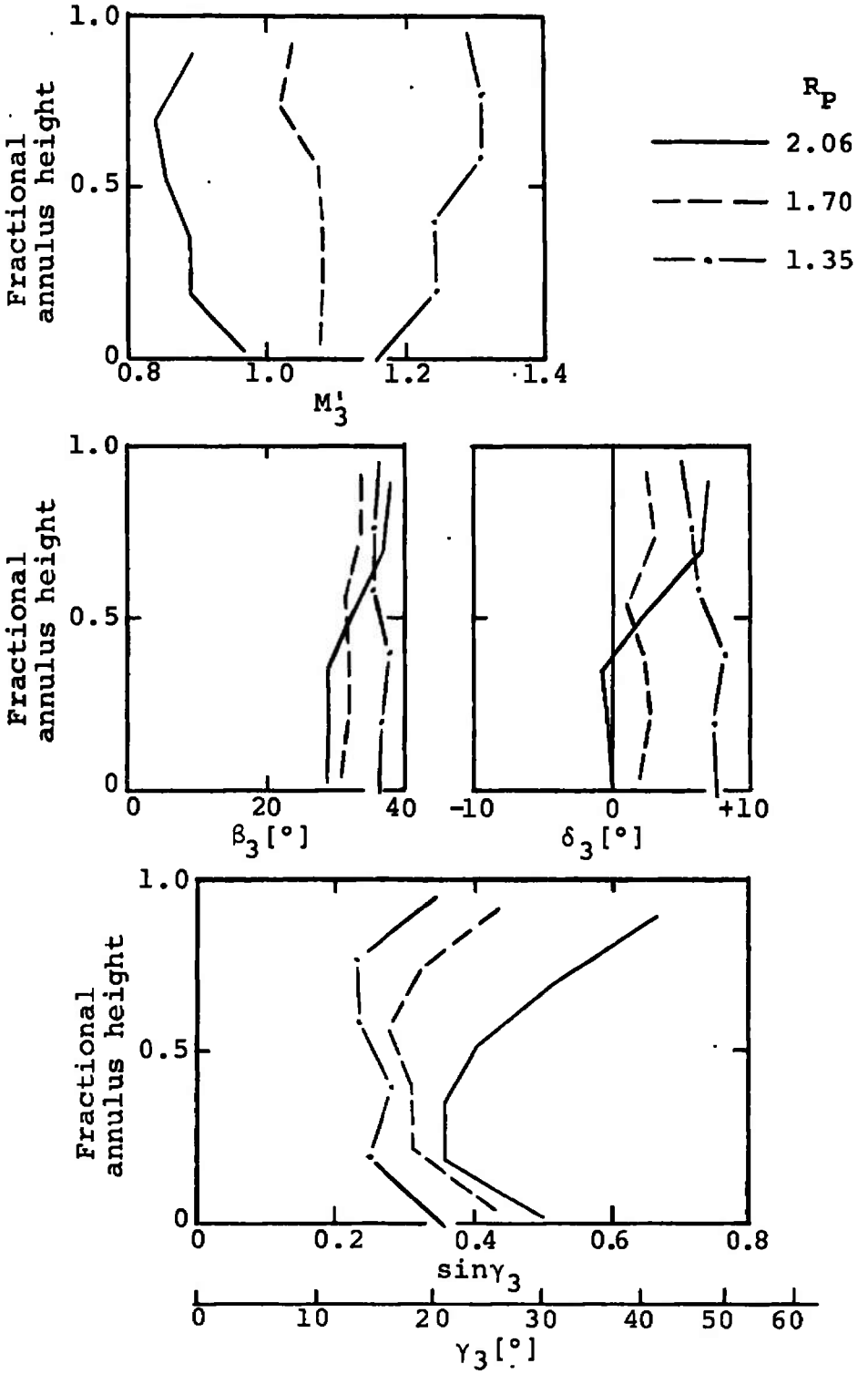


Fig. 14 Radial Variation of Solution Results for Various Absolute Total Pressure Ratios at 90-percent $N/\sqrt{\theta}$

Figure 15a shows the radial variation of the sudden area expansion loss for the same cases as shown in Fig. 14, and in Fig. 15b the one-dimensional average losses are shown for the complete speed line in comparison with the overall loss. This figure shows that the radial variation of $\omega'_{SE}$ changes considerably in function of absolute total pressure ratio, whereas the one-dimensional average of $\omega'_{SE}$ remains about constant. The fact that the average is about constant may depend on the assumption of constant weight numbers. Quasi-two-dimensional solutions for this problem suggest increasing sudden area expansion with decreasing absolute total pressure ratio (see Appendix I).

### 3.3 DISCREPANCIES IN THE RESULTS AND THEIR POSSIBLE CAUSES

Several discrepancies have been noted to result from solution of the two-dimensional sudden area expansion problem. The major discrepancy noted in the present solutions is that sudden area expansion losses become extremely large at the lower rotor speeds. This appears to be directly linked to the rapid increase noted in the pitch angle $\gamma_3$ as rotor speed decreases. It was further noted that $\gamma_3$ increases in the vicinity of the casing walls and that $\gamma_3$ is positive while the stream surface boundaries generally have negative slope at the trailing-edge plane. Such effects may occur at discrete points in the flow field, but these were not expected to be representative of the mean flow.

The result of increasing $\gamma_3$ with decreasing rotor speed may be shown to result from the particular relation between the radial and axial momentum changes. The present solution is a result of the assumption that the fluid particles, in traversing the distance between the blade trailing edge and the downstream measuring station, are affected only by the radial forces due to pressure, to centripetal acceleration, and to Coriolis acceleration. Figure 16a shows the magnitude of each of these effects for the entire control volume at each rotational speed as well as the net radial force acting on the control volume. This illustrates that in the present problem the radially inward forces due to pressure and Coriolis acceleration are larger than the outward force due to centripetal acceleration. Thus, if the fluid particles are to leave the control volume on cylindrical surfaces (i.e., $\gamma_4 = 0$), then the radial momentum at the trailing-edge plane must be directed outward.

The axial force on the fluid particles in the control volume is simply a result of the axial static pressure differential. The ratio of the resultant radial force to the axial force is shown in Fig. 16b. The ratio of momentum changes are equivalent. Thus, as rotor speed decreases,

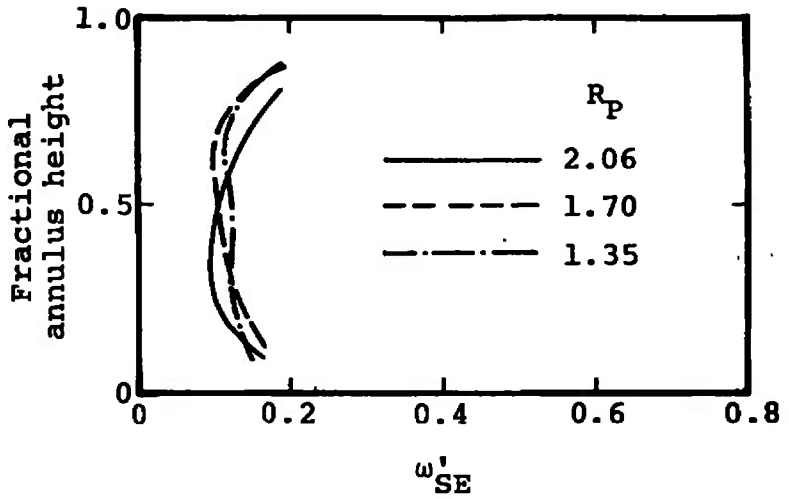


a. Radial Variation of $\omega'_{SE}$ as a Function of $R_P$

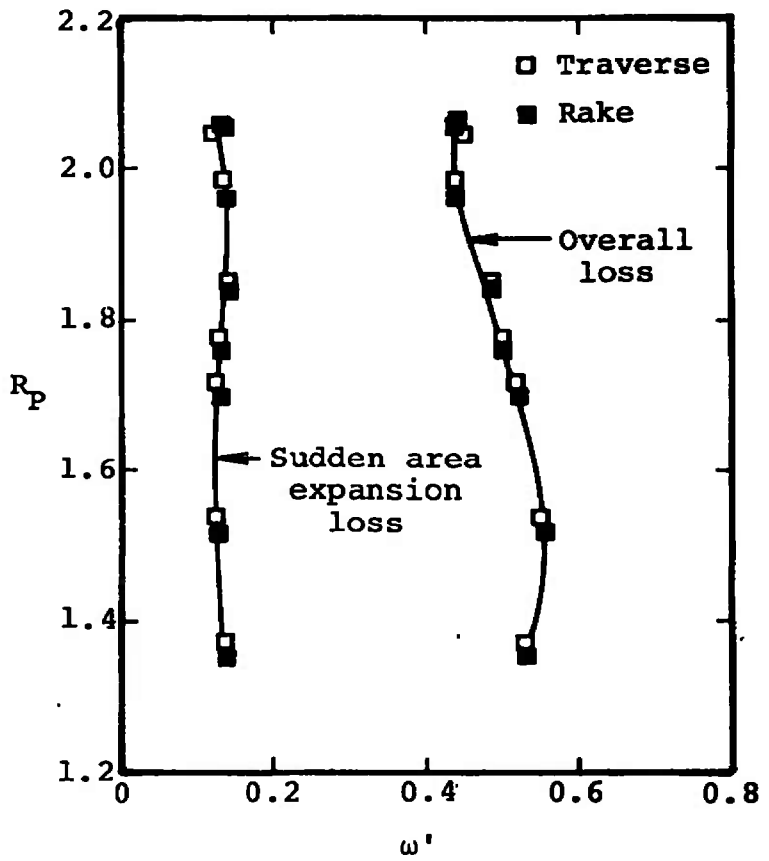


b. Variation of One-Dimensional $\omega'_{SE}$ and $\bar{\omega}'$ with $R_P$

Fig. 15 Variation of Sudden Area Expansion Loss with Absolute Total Pressure Ratio at 90-percent $N/\sqrt{\theta}$

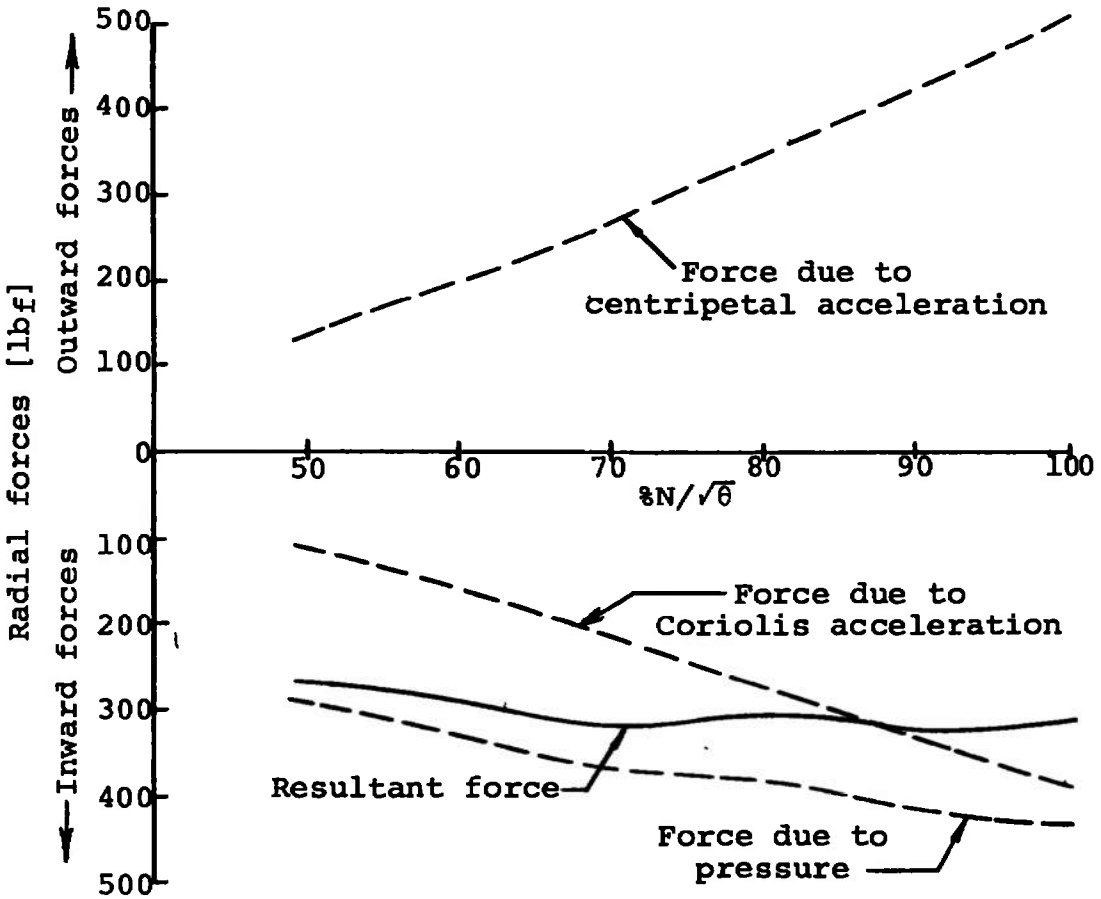


a. Variation of the Radial Force on the Control Volume as a Function of Rotor Speed

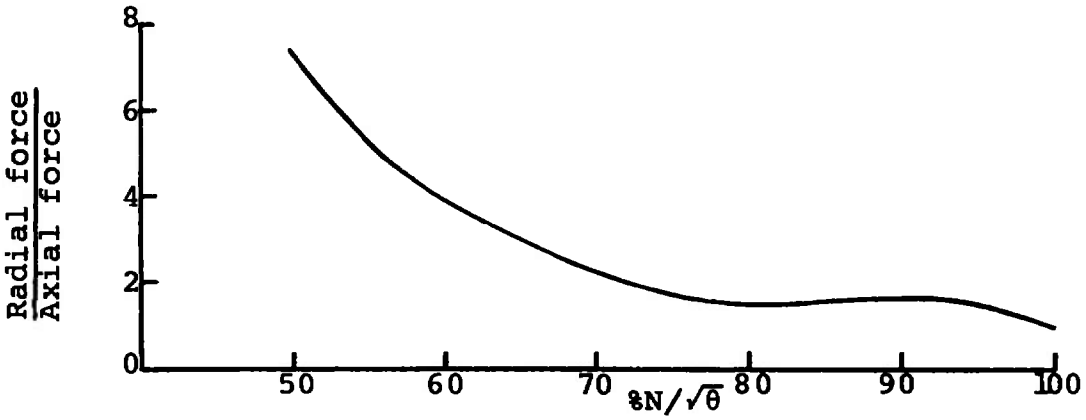


b. Relotion of the Resultant Radial Force to the Axial Farce on the Control Volume as a Function of Rotor Speed

Fig. 16 Variotion of Control Volume Forces as a Function of Rotor Speed

the radial momentum becomes increasingly larger than the value of the axial momentum. Therefore, the average radial Mach number in the control volume is predicted larger in value than the average axial Mach number, and $\gamma_3$ will increase correspondingly.

At this point, it is reasonable to question the applicability of the equations in the absolute coordinate system to this problem. The change in the absolute radial momentum depends only on the force due to the annulus pressure differential under the assumptions of steady, frictionless flow of a weightless gas. Figure 16a shows that the force due to pressure is greater than the resultant force in the relative coordinate system. Thus, the radial momentum change must be even greater in an absolute coordinate system than the present solution indicated for the relative coordinate system. Therefore, the discrepancies would be even greater.

The present solution neglects the forces due to friction, unsteady flow, and the weight of the gas. The detailed consideration of friction and unsteady flows is beyond the scope of this report, whereas the weight of the gas may still be considered negligible. However, it must be questioned whether any of these could produce the necessary correcting forces.

Of the three neglected forces, the force due to friction is the only one considered here since it is probably the largest. Although solutions have been obtained under the assumption of frictionless flow, the measurements used to obtain the solution result from a real, viscous process. Thus, the present solutions suggest no more than the distribution of the flow properties at the trailing edge if the measured flow properties resulted from an inviscid process.

Friction in the relative coordinate system will cause fluid particles near the casings to tend to adhere to the casing walls which are moving in this system. This causes the relative velocity to approach the velocity of the walls; i. e., a velocity directed opposite to the wheel rotation with the magnitude of the wheel speed. This result has two related consequences on the present solution, indicating that friction in the measurements is retained by use of the inviscid equations. First, since the radial component of the force due to Coriolis acceleration is a function of the tangential component of the relative velocity, this radial force, directed inward, increases in magnitude very rapidly as the wall is approached. The solutions for $\gamma_3$ reflect this phenomenon since $\gamma_3$ tends to increase as either casing wall is approached.

Second, the relative Mach number near the tip casing wall should increase in value, ultimately becoming equal to the Mach number of the wheel. This condition seems to be occurring in the solutions for the trailing-edge plane.

In the vicinity of the tip casing wall, the addition of the shear stress term to the radial component of the momentum equation will tend to counteract the large increase in the force due to Coriolis acceleration thereby reducing the net resultant force inward. In the vicinity of the hub wall, the local velocity gradients with respect to r are opposite to those at the tip and, thus, tend to increase the net inward force. However, if real flows are to be considered at the trailing-edge plane, it is necessary to include the boundary condition that the relative velocity tends to zero in the blade passage as the hub is approached. This significantly alters the velocity gradient at the trailing-edge plane and requires that the radial component of the force due to Coriolis acceleration approach zero. Thus, the net resultant force inward should tend to decrease at the hub.

It has been qualitatively shown that the effect of friction will tend to reduce the discrepancies noted in the solution for the radial component of the relative Mach number in the vicinity of the casing walls. This implies $\gamma_3$ may be expected to behave more rationally if the flow of a real fluid is considered. However, it is obvious in Fig. 11 that the discrepancies are continued into the main-stream flow.

In Appendix II, an attempt to estimate the effects of free turbulent flows has been made to show that free turbulent shear cannot be neglected on a stream surface. The analysis shows that the effect of friction on the radial component of the momentum equation is not sufficient to reduce the discrepancies in the center portion of the annulus. It demonstrates that the tangential component of the momentum equation is primarily affected by free turbulence. The force due to Coriolis acceleration then produces the coupling necessary to actually correct the present solutions for the radial component of velocity.

The analysis in Appendix II demonstrates that it is necessary to consider the fully three-dimensional nature of the problem. The tangential variation of velocity in the blade passage initialize irregular velocity variations in the blade wakes which result in unbalanced shear forces in the wakes. Radial secondary flows in these wakes are shown to be extremely important. The analysis is only an approximation, however, because of the severe limit in knowledge about such flow phenomenon.

Neglecting friction in compressible flows is commensurate with neglecting heat transfer in the energy equation. However, it must be pointed out that heat transfer apparently does occur from the fluid to the tip casing. This statement is based on the fact that measurements at the extra measuring plane 0.5 in. behind the rotor and the measuring plane 2.0 in. behind the rotor indicate that the entropy of the fluid decreases between these planes in the streamtube nearest the tip for all rotational speeds. Sufficient temperature measurements allowing calculation of the heat transfer rate have not been made in tests to date.

Because of the great number of assumptions incorporated into this analysis, it is impossible to point out any other single feature, besides friction, which has had a large influence on the present results. The author has investigated the consequences of errors in the weight numbers and in the specification of the static pressure at the hub in the trailing-edge plane. Such errors are relatively minor in comparison to the gross error introduced by neglecting friction. Certain other assumptions, such as straight-line static pressure variation radially across the annulus, the conical form of the stream surfaces, and others which purport to estimate unmeasured flow properties, may be deemed critical when it is possible to include friction in the present analysis. The interpretation of the existing measurements may ultimately be questioned. It should be recalled, however, that frictional effects were depicted as large in Appendix II under the basic assumption that radial velocity components were relatively large in the blade wakes; i.e., consideration of secondary flows becomes an essential part of the solution. Furthermore, it is the variation of flow properties from blade to blade that initiates the velocity gradients of sufficient magnitude to produce the large frictional effects. Thus, it can be concluded that the sudden area expansion problem for the blunt trailing-edge rotor is a fully three-dimensional problem which will not be completely understood without a general and complete three-dimensional analysis.

## SECTION IV
## CONCLUDING REMARKS

The sudden area expansion process is fully three-dimensional in rotor flows. Tangential blade-to-blade flow property variations and radial velocities in the blade boundary layers and wakes, indicative of secondary flows, play an extremely important part in determining the flow development. At present, these are not well enough understood to allow any more than a qualitative estimate of their effects.

This report has investigated the sudden area expansion process as a quasi-three-dimensional, frictionless, adiabatic flow process by the use of the streamtube approximation, and it has been demonstrated that the real flow process cannot be approximated in such a manner. The general behavior of the solutions for the relative Mach number and the relative yaw angle at the trailing edge may be considered quite good; however, the behavior of the solutions for the relative pitch angle must be considered very poor as a description of the average flow process.

The reasons for the difficulties are relatable to neglecting friction. Friction at solid boundaries is important, but it is shown that the primary effect of friction on a problem approached by the streamtube approximation is relatable to free turbulent shear. Velocity profiles are highly nonaxisymmetric at the trailing-edge plane because of the blade element curvature. This results in unbalanced shear forces in the blade wakes. The solutions of the problem considered in this report indicate that these effects must be accounted for. In addition, sizable radial velocities in the wakes are also required to account for the discrepancies noted in the present solutions.

It is believed that the discrepancies occurred because real-flow measurements were used with the ideal-flow equations. Measurements were available to describe the flow properties downstream of the rotor, and the flow conditions at the rotor trailing edge were demanded from the inviscid flow equations. The resulting solutions can only be interpreted as the conditions at the trailing edge if the process leading to the measured data were inviscid.

The quasi-two-dimensional equations lead to more reasonable results for sudden area expansion flow process. This result can only be related to the real flow process if it is hypothesized that neglecting friction and radial secondary flows are at least partially compensating assumptions. It should be emphasized that the solutions of the quasi-two-dimensional equations will lead to incorrect results if the streamtube assumption is used.

The development and form of the quasi-three-dimensional equations show that it is not currently possible to solve the problem for the flow conditions downstream of the rotor if only the conditions at the rotor trailing edge are supplied. The solution requires some knowledge of the flow process. In particular, it requires the static pressure development along the annulus walls as well as some information about the volume integrals of the forces due to Coriolis and centripetal acceleration. Only experience with the solution of the equations in a form similar to the present analysis will lead to knowledge necessary to solve the inverted problem.

An experimental and theoretical program is proposed to continue study of this problem. Some suggested experiments are:

1. Sudden area expansion in pipe flows, similar to those of Ref. 12, to include a sufficient variety of area ratios and a further investigation of the effect of geometry over the complete range of initial Mach number (0 to 1.0) and possibly varying back pressure when the inlet flow is choked and the downstream flow becomes supersonic. Such an investigation is aimed at determining the static pressure on the trailing surface. The theory for this problem is simple for frictionless flow and should agree very well with experimental results.
2. Flows in cascades designed to produce symmetrical outlet flows from each passage. The theory is still one-dimensional and the effects of shear stress are probably still negligible, but the objective is to determine the effects of wake flows on the trailing-surface static pressure. Studies of free turbulence may be of interest to determine wake development.
3. Flows in cascades of curved surface blading producing tangential gradients in the initial flow before the sudden area expansion. The theory becomes two-dimensional, and the objective is to determine the applicability of basically one-dimensional theories such as Ref. 7. Discrepancies due to shear stress are expected to become increasingly important. Studies of free turbulence should definitely be attempted.
4. Flows through curved blades in annular cascade to determine the effect of radial pressure gradients. The theory must become completely three-dimensional now, and very significant discrepancies should occur if the effect of shear stress is neglected in the analysis. Wake studies become extremely important here since this is the simplest case through which experiments can demonstrate the effects of radial forces on the development of the wakes.
5. Flows in rotors. At present, because of the lack of techniques for measuring flow properties in the rotating system, this study must be completely theoretical. All the information gathered by the previous studies may

still be insufficient except at very low rotor speeds where the forces due to Coriolis and centripetal acceleration may be considered negligible. This study is intimately connected with a study of the flow development through the blading since the advantage of knowing the initial conditions before the sudden area expansion process does not exist in the case of rotor flows.

## REFERENCES


1. Members and Staff of the Lewis Research Center, Cleveland, Ohio. "Aerodynamic Design of Axial Flow Compressors, Revised." National Aeronautics and Space Administration SP-36, Washington, D. C. 1965.
2. Carman, C. T., Myers, J. R., Wennerstrom, A. J., and Steurer, J. W. "Experimental Investigation of Two Blunt Trailing Edge Supersonic Compressor Rotors of Different Blade Thicknesses and with Circular Arc Camber Line." AEDC-TR-68-197 (AD674743), September 1968.
3. Carman, C. T., Myers, J. R., and Wennerstrom, A. J. "Experimental Investigation of Two Blunt-Trailing-Edge Supersonic Compressor Rotors of Different Blade Thicknesses and with Polynomial Camber Line." AEDC-TR-68-251 (AD681488), January 1969.
4. Johnson, E. G., von Ohain, H., Lawson, M. D., and Cramer, K. R. "A Blunt-Trailing-Edge Supersonic Compressor Blading." WADC TN 59-269, 1959.
5. Fejer, A. A., Heath, G. L., and Driftmeyer, R. T. "An Investigation of Constant Area Supersonic Flow Diffusion." ARL 64-81. May 1964.
6. Heath, G. L. "An Investigation of Diffusion of Supersonic Flows in Curved Constant Area Passages." ARL 65-179. September 1965.
7. Wennerstrom, A. J. "Flow Tables for Air ($\gamma$ = 1.4) Passing an Abrupt Area Increase Oblique to the Flow Direction." ARL 64-10. January 1964.

8. Salvage, J. W. "Investigation of the Flow through Supersonic Compressor Rotors of Blunt-Trailing-Edge Blade Design." Master of Science Thesis, University of Tennessee Space Institute, Tullahoma, Tennessee, June 1970.

9. Wennerstrom, A. J. and Olympios, S. "A Theoretical Analysis of the Blunt-Trailing-Edge Supersonic Compressor and Comparison with Experiment." ARL 66-0236, November 1966.

10. Olympios, S. "Numerical Analysis of the Blunt-Trailing-Edge Supersonic Compressor." ARL 66-0189, September 1966.

11. Vavra, M. H. Aero-Thermodynamics and Flow in Turbomachines. New York, John Wiley & Sons, Inc. 1960.

12. Shouman, A. R. and Massey, J. L., Jr. "Stagnation Pressure Losses of Compressible Fluids through Abrupt Area Changes Neglecting Friction at the Walls." Paper No. 68-WA/FE-46 presented at the 89th ASME Winter Annual Meeting and Third Energy Systems Exposition. New York, N. Y., December 1-5, 1968.

13. Schlichting, H. Boundary Layer Theory. Translated from the German by J. Kestin. Fourth Edition. New York, McGraw-Hill Book Company, Inc. 1960.

14. Lin, C. C. (ed.). Turbulent Flows and Heat Transfer. Vol. V of High Speed Aerodynamics and Jet Propulsion. 12 vols. Princeton, New Jersey. Princeton University Press, 1959.

15. Torda, T. P., Ackermann, W. O., and Burnett, H. R. "Symmetric Turbulent Mixing of Two Parallel Streams." Journal of Applied Mechanics, Vol. 20, pp. 63-71, March 1953.

# APPENDIXES

I. THE QUASI-TWO-DIMENSIONAL APPROACH
II. AN ESTIMATE OF THE EFFECT OF FREE TURBULENT FLOWS ON THE STREAMTUBE APPROXIMATION

# APPENDIX I
# THE QUASI-TWO-DIMENSIONAL APPROACH

## FORMULATION OF THE PROBLEM AND REVIEW OF A RELATED EXPERIMENT

In an effor to establish the approximate order of magnitude of loss due to the sudden expansion process, the analysis in Ref. 7 used the momentum theorem with certain simplifying assumptions. The main assumptions were:

1. The flow is steady, adiabatic, and axisymmetric in the absolute frame of reference with concentric cylindrical stream surfaces.
2. Friction is neglected.
3. Radial secondary flows are neglected.

The loss in total pressure then becomes a function only of the area ratio and the component of the Mach number in the direction of the area increase. Thus a fully three-dimensional problem is reduced to solution in one dimension. The axial component of the momentum equation, neglecting the shear stress term and the weight of the gas, is used in the form

$$\rho_4 W_{z4}^2 A_4 - \rho_3 W_{z3}^2 A_3 = p_3 A_3 - p_4 A_4 + p_3'(A_4 - A_3) \tag{I-1}$$

where $p_3'$ represents the pressure on the surface of the blade trailing edges. In Ref. 7, $p_3'$ is assumed equal to $p_3$ which leads to

$$p_3(A_4 - A_3) + p_3 A_3 + \rho_3 W_{z3}^2 A_3 - p_4 A_4 - p_4 W_{z4}^2 A_4 = 0$$

By using the one-dimensional continuity equation, the energy equation, and the equation of state to eliminate $p_4/p_3$, the equation above becomes

$$\frac{\frac{A_4}{A_3} + \kappa M_3'^2 \cos^2 \beta_3}{M_3' \cos \beta_3 \left(1 + \frac{\kappa - 1}{2} M_3'^2\right)^{\frac{\kappa}{\kappa-1}}} = \frac{1 - \kappa M_4'^2 \cos^2 \beta_4}{M_4' \cos \beta_4 \left(1 - \frac{\kappa - 1}{2} M_4'^2\right)^{\frac{1}{\kappa-1}}} \tag{I-2}$$

If station 3 is assumed to be located at a plane such that the flow has not yet experienced the sudden area expansion and such that the rotor may not further impart momentum to the flow, then substitution of the two-dimensional flow triangle relations into the tangential component of the momentum equation leads to

$$\frac{M_3' \sin \beta_3}{\left(1 + \frac{\kappa - 1}{2} M_3'^2\right)^{\frac{1}{2}}} = \frac{M_4' \sin \beta_4}{\left(1 + \frac{\kappa - 1}{2} M_4'^2\right)^{\frac{1}{2}}} \tag{I-3}$$

since the stream surfaces are assumed cylindrical. Thus Eqs. (I-2) and (I-3) relate the variables $A_4/A_3$, $M_3'$, $\beta_3$, $M'_4$, and $\beta_4$. Any three of these may be chosen as knowns and the other two may then be determined uniquely. The static pressure ratio and the total pressure recovery are then determined from the continuity equation in the form:

$$\frac{p_4}{p_3} = \frac{A_3}{A_4} \frac{M_3' \cos \beta_3}{M_4' \cos \beta_4} \left[\frac{1 - \frac{\kappa - 1}{2} M_3'^2}{1 - \frac{\kappa - 1}{2} M_4'^2}\right]^{\frac{1}{2}} \tag{I-4}$$

$$\frac{p_4}{p_3} = \frac{A_3}{A_4} \frac{M_3' \cos \beta_3}{M_4' \cos \beta_4} \left[\frac{1 + \frac{\kappa - 1}{2} M_4'^2}{1 + \frac{\kappa - 1}{2} M_3'^2}\right]^{\frac{\kappa + 1}{2(\kappa - 1)}} \tag{I-5}$$

The one-dimensional approximation is valid as long as no cross-flow components exist; however, the approximation may be applied to real flows if the velocity profiles are fully developed. This means that integration of shear stress over a control surface perpendicular to the mean flow direction must be zero; then neglecting friction merely requires that friction along solid boundaries be negligible.

These considerations imply that the quasi-two-dimensional equations are best applied to the entire annulus and not to individual streamtubes. The results for an extension of the analysis presented in the main body of this report affirm this conclusion and point out that tangential blade-to-blade velocity variations produce large shear forces in the blade wakes that must be accounted for in the streamtube approximation.

Under these circumstances, the best approximation seems to be calculation of the sudden area expansion loss based on average flow properties for the entire annulus and, assuming the same resulting loss, occurs in each streamtube.

In Ref. 12, an attempt is made to correlate empirically the value of $p_3'$ in Eq. (I-1) with the actual measured losses in one-dimensional pipe flow (i.e., $\beta_j = 0$, $j = 3, 4$) for both sudden area expansion and contraction. The assumptions of this reference and those of Ref. 7 are otherwise the same. The average base pressure for sudden area expansion and contraction is measured experimentally, and the actual losses are compared with those determined analytically using the average measured

base pressure. A good correlation results indicating that use of Eq. (I-2) yields somewhat lower losses than those which occur in experiment. If $p_3'$ is left in Eq. (I-1), an equation similar to Eq. (I-2) results.

$$\frac{\frac{p_3'}{p_3}\left(\frac{A_4}{A_3}-1\right)+1+\kappa M_3'^2\cos^2\beta_3}{M_3'\cos\beta_3\left(1+\frac{\kappa-1}{2}M_3'^2\right)^{1/2}}=\frac{1+\kappa M_4'^2\cos^2\beta_4}{M_4'\cos\beta_4\left(1+\frac{\kappa-1}{2}M_4'^2\right)^{1/2}} \qquad (I\text{-}2')$$

Since Eq. (I-3) remains unchanged, the Eqs. (I-2′) and (I-3) relate the variables $A_4/A_3$, $M_3'$, $\beta_3$, $M_4'$, $\beta_4$, and $p_3'/p_3$. Thus, it is necessary to know four of these quantities before the other two may be determined uniquely. However, if sufficient data are available to establish an accurate correlation of $p_3'/p_3$ in function of, say, $A_4/A_3$ and $M_3' \cos \beta_3$, then again selection of any three of the variables as known quantities allows unique solution for the remaining two variables.

In Ref. 12, two area ratios (outlet area/inlet area) were tested, 2.25 and 4.00, using both circular and square ducting. Definite dependence of base pressure on geometry was noted. The results for expansion indicate that, as the Mach number before expansion approaches sonic, as much as 10-percent error may be made in the calculation of the total pressure recovery factor through the use of an equation like Eq. (I-2) rather than Eq. (I-2′) at an area ratio of 2.25 and about 15-percent error occurs in the case of an area ratio of 4.00. The difference in the results of Eqs. (I-2) and (I-2′) decreases as Mach number decreases.

These experiments indicate that some error is made in the use of Eq. (I-2); i.e., by the assumption that $p_3' = p_3$ and that the error decreases as both the Mach number before expansion and the area ratio decrease. Insufficient data exist at the present to allow correlation of $p_3'$ for area ratios useful in this investigation (1.37 to 1.83).

It might be useful to make additional tests extending the data of Ref. 12 to smaller area ratios so that Eq. (I-2′) may be used in the one-dimensional analysis of the blunt trailing-edge blading. The reasons against such a program include the fact that the flow in an apparatus like that of Ref. 12 may be quite different from that experienced by a blunt trailing-edge stator and certainly must be different from the flow experienced by a rotor due to the peculiarities of the rotating flow field. However, until flow measurement in a rotating flow field becomes practical, researchers must be satisfied with experiments performed in a nonrotating field conscientiously applied as guides for describing the flow in a rotating coordinate system. Certainly refined experiments similar to that in Ref. 12 should be attempted for flow in annular

cascades when the problem is critically important to the analysis, but for the moment, the simplest experiment should be attempted to determine the order of magnitude of the error made in using Eq. (I-2) rather than Eq. (I-2′).

## METHODS OF SOLUTION AND RESULTS OF CALCULATION

The particular use of Eqs. (I-2) to (I-5) for the calculations of this report requires some further rearrangement of those equations. Measurements at the downstream measuring plane may be used to yield average values of $M_4'$ and $\beta_4$ for the annulus. Thus, one of the remaining three variables, $A_4/A_3$, $M_3'$, or $\beta_3$, must be specified in order to determine a solution of Eqs. (I-2) and (I-3). It is immediately obvious that $M_3'$ cannot be specified and that $A_4/A_3$ should not be specified since one of the objectives of the calculation was to determine the effective flow area at the trailing edge. Under the basic assumption of the applicability of these equations, it is necessary that the flow should not be separated at either the trailing-edge plane or the downstream measuring plane. Therefore, the flow angle ($\beta_3$) should be reasonably close to the exit blade angle ($\beta_3'$). Their equivalence is assumed for the calculations for Method One below.

A second possible method of calculation requires somewhat more leniency in both data interpretation and the assumptions. This method involves the specification of the static pressure ratio accomplished by the process. Measurements of static pressure are made along the hub and tip casing walls between the rotor trailing-edge plane and downstream measuring stations except at the hub wall in the trailing-edge plane where measurement is not physically possible. If this static pressure were available together with the static pressure measurement at the rotor tip, then a linear variation could be used to approximate the static pressure at any radius. Use is made of the Legrange interpolation formula and all static pressures measured on the hub wall to extrapolate for the hub wall static pressure at the rotor trailing-edge plane. The closest measured pressure is 0.25 in. downstream of the rotor trailing edge, and this is one of five used in the extrapolation, the most distant being at the plane of the downstream flow measurements. This is Method Two described below.

### Description and Results of Method One

The critical Mach number, given by

$$M^{*2} = \frac{\frac{\kappa - 1}{2} M^2}{\frac{\kappa - 1}{2} M^2 + 1}$$

may be used to put Eq. (I-3) into the form

$$M_3'^* \sin\beta_3 = M_4'^* \sin\beta_4$$

which, for given $\beta_3$, $\beta_4$, and $M_4'$, may be solved for $M_3'^*$ leading to $M_3'$. Equation (I-2) may then be solved for $A_4/A_3$. These computations yield sufficient information to determine the static and total pressure ratios from Eqs. (I-4) and (I-5). The relative total pressure loss attributable to the sudden area expansion process is then given by

$$\omega'_{SE} = \frac{P'_3 - P'_4}{P'_2 - p_2}$$

The average one-dimensional losses are plotted versus absolute total pressure ratio in Fig. I-1 for rotor R1C2.

Careful examination of Fig. I-1 shows that sudden expansion loss generally increases as the absolute total pressure ratio decreases for constant speed operation except in the case of design speed operation. Since maximum pressure ratio implies maximum diffusion to a minimum passage exit Mach number, most of the results show reasonable variation for the loss due to the sudden area expansion flow process. As the pressure ratio is decreased at constant wheel speed, the trailing-edge Mach number increases, implying that the level of sudden expansion loss should increase.

However, each of the curves for design speed operation exhibit an abrupt decrease in loss at minimum total pressure ratio. This result of the calculations can be directly linked to the occurrence of a sharp increase in the axial Mach number downstream of the rotor when back pressure is reduced to a minimum. The calculated trailing-edge relative Mach numbers tend to show that the flow through the rotor has actually been accelerated for these minimum-pressure-ratio operating conditions. Static pressure measurements at the rotor tip also tend to confirm the acceleration at minimum pressure ratio (see Refs. 2 and 3 and Fig. 26 of Ref. 8).

#### Description and Results of Method Two

Equation (I-4) may be solved for $A_4/A_3$ and used to eliminate the area ratio from Eq. (I-2). Then substitution of Eq. (I-3) leads to

$$\tan\beta_3 = \frac{\kappa M_4'^2 \sin\beta_4 \cos\beta_4}{1 - \frac{p_3}{p_4} + \kappa M_4'^2 \cos^2\beta_4}$$

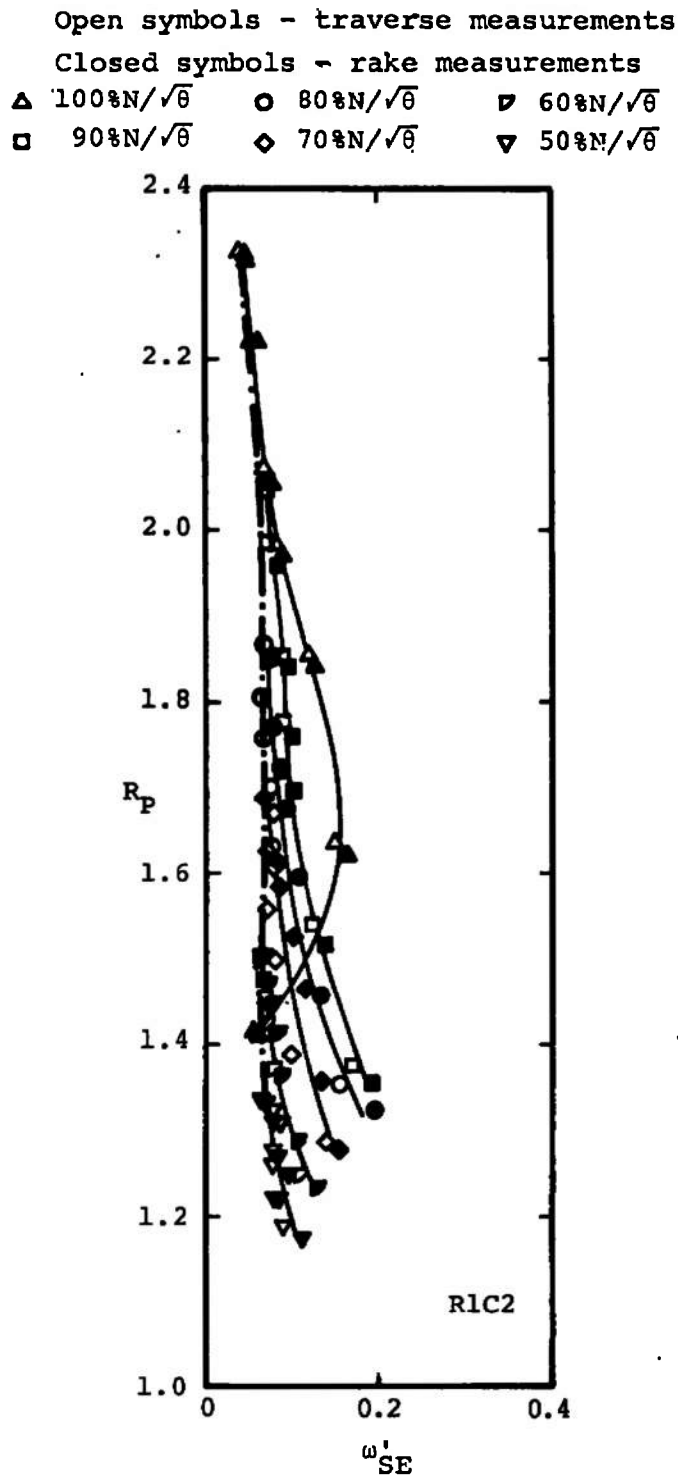


Fig. I-1 Sudden Area Expansion Loss Calculated by Method One versus Absolute Total Pressure Ratio

from which $\beta_3$ may be calculated when $p_3/p_4$, $M_4'$, and $\beta_4$ are given. The calculation procedure is then similar to Method One leading to the calculation of the relative total pressure ratio by Eq. (I-5). The average one-dimensional sudden expansion losses are plotted versus absolute total pressure ratio in Fig. I-2 for rotor R1C2.

The general trends of variation of sudden expansion loss for each speed line in Fig. I-2 is very similar to that observed in Fig. I-1; i.e., increasing loss with decreasing pressure ratio. The calculation results must then be considered to yield plausible results. However, it is noted that the magnitude of sudden expansion loss is considerably reduced with the use of Method Two.

Figure I-3 shows the variation of the deviation angle ($\delta_3$) at the trailing-edge plane in function of absolute total pressure ratio for selected wheel speeds. The deviation angle is defined as the difference between the flow direction and the blade angle, both measured in a plane perpendicular to the radial direction. The deviation angle is a measure of the flow guidance accomplished by the blading. In Method One, flow guidance was assumed perfect; i.e., $\delta_3$ was identically zero.

## COMPARISON OF METHODS

In this section, it is intended to compare and contrast the results of the three methods (two quasi-two-dimensional methods and the quasi-three-dimensional method) to determine which, if any, can be used to approximate the losses due to the sudden area expansion process that occurs as the flow leaves the rotor blade passages.

From the discussion of Fig. 13, it must be concluded that sudden area expansion loss is grossly over-estimated by the quasi-three-dimensional calculations at low rotor speed; however, the possibility of reasonable predictions at high speeds must be considered. The behavior of the solutions at 90-percent $N/\sqrt{\theta}$ in function of absolute total pressure ratio shown in Figs. 14 and 15 may be reasonable even though the trend of loss variation is not substantiated by the quasi-two-dimensional results. The single feature which must lend doubt to the accuracy of the solutions is the large values of $\gamma_3$ and the fact that, in most cases, the flow at the blade trailing edge is not directed paralled to the bounding stream surfaces. This occurrence has been directly linked to neglecting viscous shear. (It might be commented here that an attempt has been made to force solution of the equations to negative values of $\gamma_3$. Such solutions were not possible, indicating that the inviscid equations could not be solved if $\gamma_3$ were approximated by the local slope of the stream surfaces at the trailing-edge plane.)

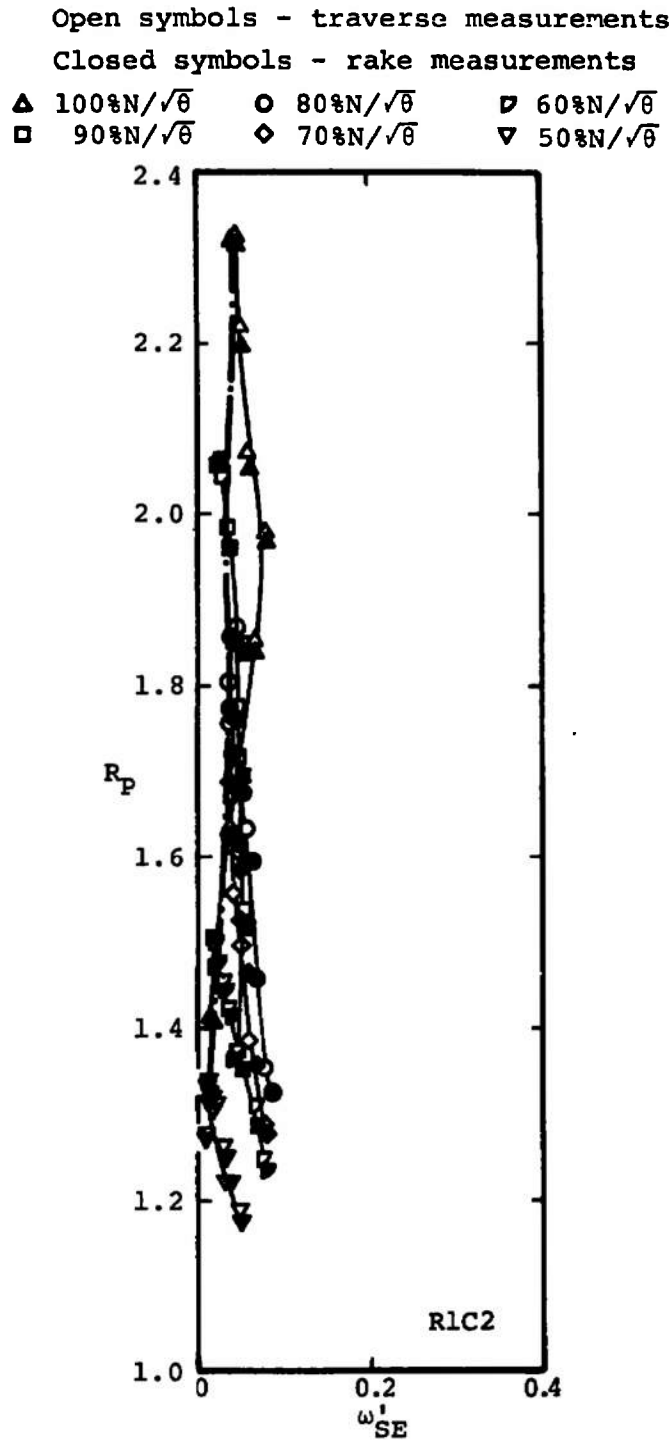


Fig. 1-2 Sudden Area Expansion Loss Calculated by Method Two versus Absolute Total Pressure Ratio

Open symbols - traverse measurements
Closed symbols - rake measurements

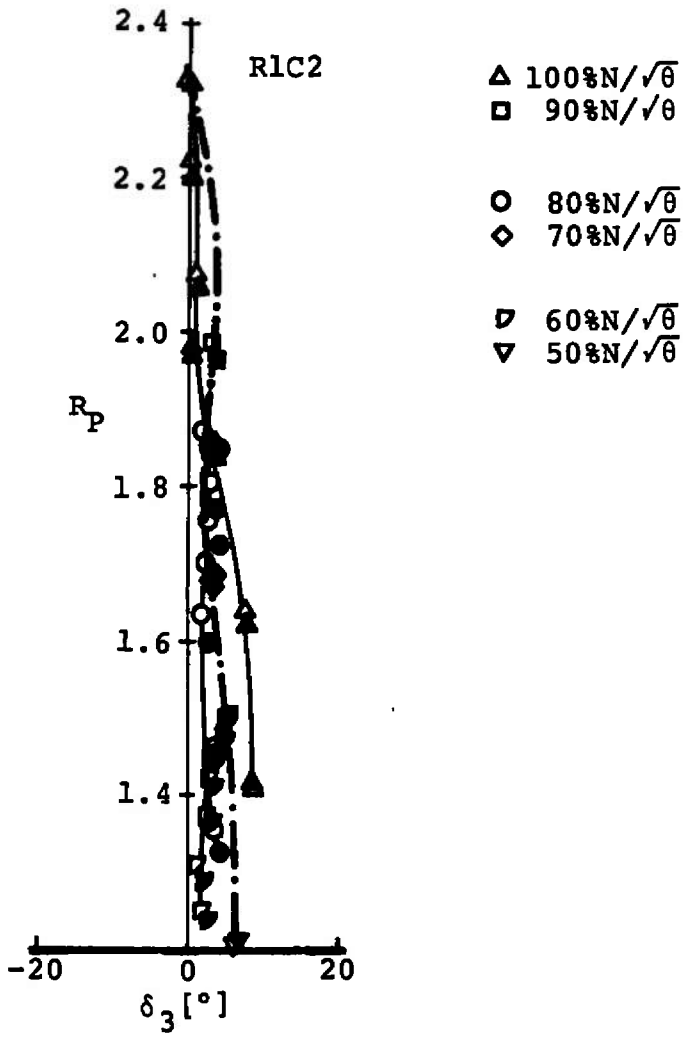


Fig. I-3 Variations of the Deviation Angle Calculated by Method Two as a Function of Absolute Total Pressure Ratio

Since much of the effort to correct the quasi-three-dimensional solutions in the previous section was directed toward reduction of the radial velocity, it appears reasonable that the quasi-two-dimensional solutions which ignore the existence of a radial component in velocity should give more reasonable results. However, neglecting shear stress would be just as critical in the case of the quasi-two-dimensional solutions as it is in the case of the quasi-three-dimensional solutions if the streamtube approximation were used.

An approximation similar to the quasi-two-dimensional method may be attempted using the quasi-three-dimensional equations. This is accomplished by solving the entire annulus as if it were the initial streamtube (see Section 2.7). Essentially, this means all solution variables are assumed constant at the trailing-edge plane, but that both radial and tangential components of velocity are allowed to occur. The results for sudden area expansion loss are shown in comparison to the completely quasi-three-dimensional results, the quasi-two-dimensional results by both methods, and the measured overall loss in Fig. I-4. This method produces a significant reduction in the estimated loss but not nearly sufficient to consider it a correct approximation to the actual loss at low rotor speeds.

Comparison of the two quasi-two-dimensional methods reveals that Method One generally yields higher relative total pressure losses for the process and smaller values for the flow angle, static pressure, and flow area at the trailing-edge plane. The tendancy of increasing sudden expansion loss with decreasing absolute total pressure ratio for constant speed operation is apparent in both quasi-two-dimensional methods. This is more consistent with ideas of how flow in the passage behaves than the results of the quasi-three-dimensional analysis which suggests that the loss is constant.

Considering the relation between the two quasi-two-dimensional methods it may be concluded that the results would be the same by each method if:

1. The flow were assumed to have a small, generally positive deviation from the blade angle at the trailing edge for use in Method One, or
2. The extrapolation procedures necessary for Method Two were to have produced a hub wall static pressure at the trailing edge that was too large, or both of these.

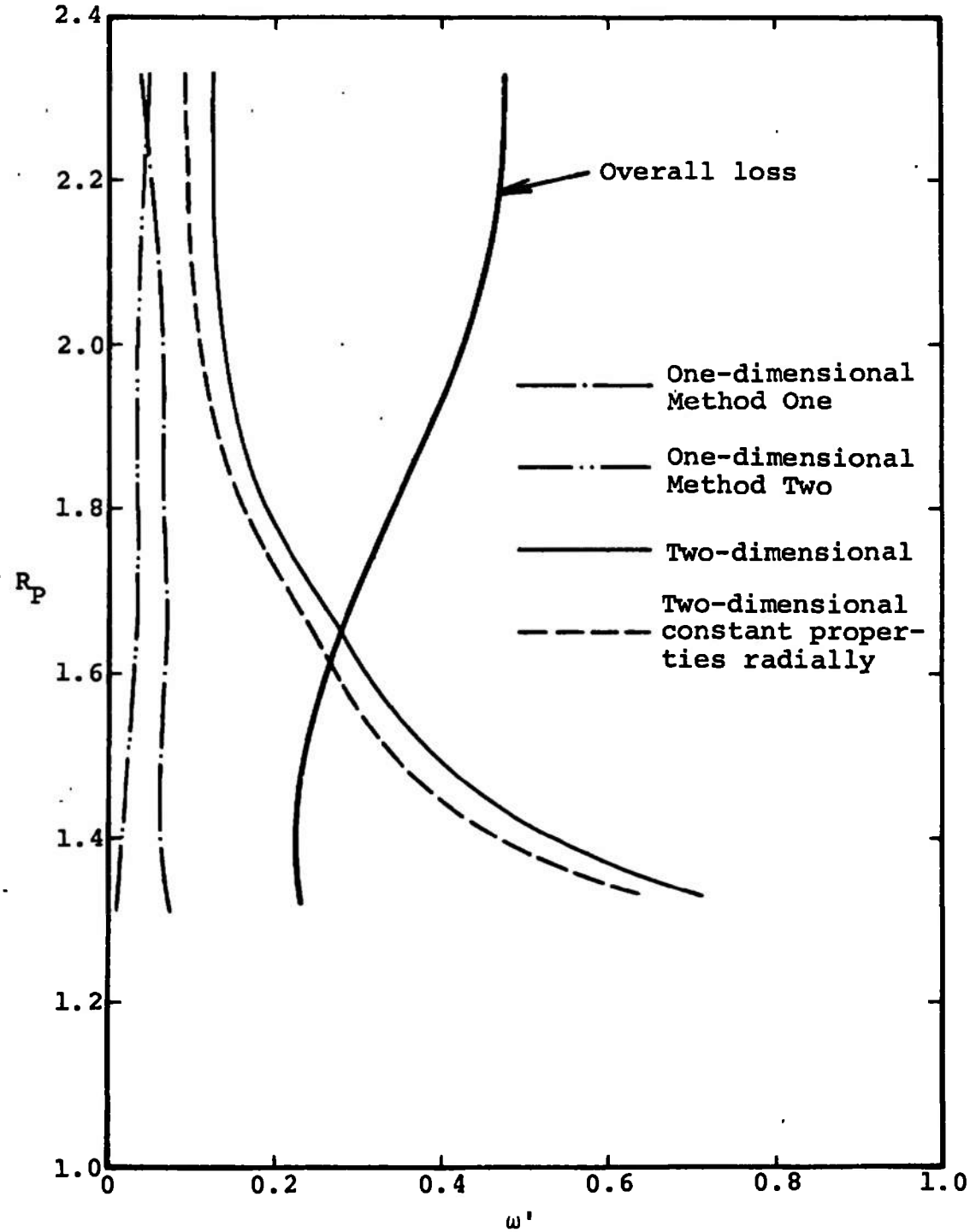


Fig. I–4 Comparison of the Measured Overall Relative Total Pressure Loss with the Results of various Methods Predicting Sudden Area Expansion Loss

Either of these alternatives could have occurred for any given set of measured conditions downstream of the rotor, thereby making the choice between them quite arbitrary. Ultimately, the decision as to which method is more realistic for this problem can be made only in connection with the flow model as a whole. This report does not deal with the consequences of selecting the calculation procedure; however, some comments on these two alternatives may be made here.

First, some deviation from perfect flow guidance certainly must be expected at the trailing edge. Its magnitude could be calculated from Method Two if the trailing-edge static pressure were known with some certainty and, of course, if the assumptions of the analysis were obeyed in reality. Second, it is felt that the extrapolated static pressure on the hub wall is not predicted too large. As a matter of fact, in a small number of cases (actually amounting to only 1 percent of the total number), the extrapolated pressure was too small to allow solution of the equations.

This qualitative analysis suggests that, if the assumptions of the theory are obeyed, Method Two is probably superior to Method One. If the assumptions are not obeyed, in particular, if the flow contains radial flow components, then the results of the quasi-three-dimensional analysis suggests that Method One is more reasonable since it predicts larger losses in relative total pressure.

## APPENDIX II
## AN ESTIMATE OF THE EFFECT OF FREE TURBULENT FLOWS ON THE STREAMTUBE APPROXIMATION

According to Ref. 13 and others, turbulent boundary layer theory assumes that the shear stress may be given by

$$\tau = \rho(\nu + \epsilon) \frac{\partial \bar{u}}{\partial y}$$

where $\nu$ is the laminar kinematic viscosity, $\epsilon$ is the virtual kinematic viscosity of turbulent flows, $\bar{u}$ is the local time-averaged velocity of the mean motion, and y denotes the direction transverse to the mean motion. For free turbulent flows, such as jets and wakes, $\nu$ may be neglected in comparison to $\epsilon$. From page 481 of Ref. 13,

> ...L. Prandtl assumed that the dimensions of the lumps of fluid which move in a transverse direction during turbulent mixing are of the same order of magnitude as the width of the mixing zone.... The virtual kinematic viscosity, $\epsilon$, is now formed by multiplying the maximum difference in the time-mean flow velocity with a length which is proportioned to the width, b, of the mixing zone. Thus
>
> $$\epsilon = \kappa_1 b (\bar{u}_{max} - \bar{u}_{min}) \qquad \text{(II-1)}$$
>
> Here $\kappa_1$ denotes a dimensionless number to be determined experimentally.

The value of $\epsilon$ is often assumed to remain constant over the whole width of the wake at every cross section; and, in the case of plane wakes, Ref. 14 demonstrates that $\epsilon$ is constant, independent of the distance from the body, as long as velocity profile similarity exists. The latter result is then valid only at large distances from the wake-producing body, whereas the former assumption may be corrected by introducting an intermittency factor accounting for the periods of time in which turbulence occurs at a particular point in the flow field.

Most theoretical wake flow studies have been applied to incompressible flows with negligible pressure gradients, and these have been successful only in application to large distances from the body. In application to the present problem, Eq. (II-1) for $\epsilon$ and the resulting equation

$$\tau = \rho \kappa_1 b (\bar{u}_{max} - \bar{u}_{min}) \frac{\partial \bar{u}}{\partial y} \qquad \text{(II-2)}$$

for shear stress will be used to arrive at estimates for these quantities in the vicinity of the rotor trailing edges. The quantity ($\kappa_1$) is assumed a constant, but in reality it may depend on the type of problem to which the approximation for $\epsilon$ is being applied as well as on the distance from the body at which $\tau$ is being calculated.

Certain further assumptions must be made for the present application. The solutions of the quasi-three-dimensional sudden area expansion problem make it possible to estimate the average relative velocity and density at the plane of the rotor trailing edge. The variation of these quantities with percent of design rotor speed is shown in Fig. II-1 (top). By assuming that the wake width (b) may be approximated by the blade trailing-edge thickness (th) and that the velocity difference is given by

$$u_{max} - u_{min} = W_3 - 0$$

then

$$\frac{\epsilon}{\kappa_1} \approx r_{ref} \left(\frac{th}{r}\right) W_3 \qquad \text{(II-3)}$$

where $r_{ref}$ is the radius of the blading reference profile. The results of this calculation are shown in Fig. II-1 (middle).

Several examples using the approximation for $\epsilon$ expressed by Eq. (II-1) are given in Ref. 13. The value of the constant apparently depends on the problem. The following results have been noted:

$$\kappa_1 = \begin{cases} 0.014 \text{ free-jet boundary} \\ 0.047 \text{ quadi-three-dimensional wake} \\ 0.0333 \text{ wake behind row of bars} \\ 0.0185 \text{ two-dimensional jet} \\ 0.0128 \text{ circular jet} \end{cases}$$

According to Ref. 15, $\kappa_1$ may be on the order of 0.1 for the case of the mixing of parallel streams when initial velocity gradients on the body are taken into account.

For the purposes of this investigation, a value of 0.0333 is chosen for $\kappa_1$ because the wake behind a row of bars best represents the problem and because it is convenient to state that the final results may be too small or too large by a factor of three. Then, $\epsilon$ is given by the right-hand scale of Fig. II-1 (middle).

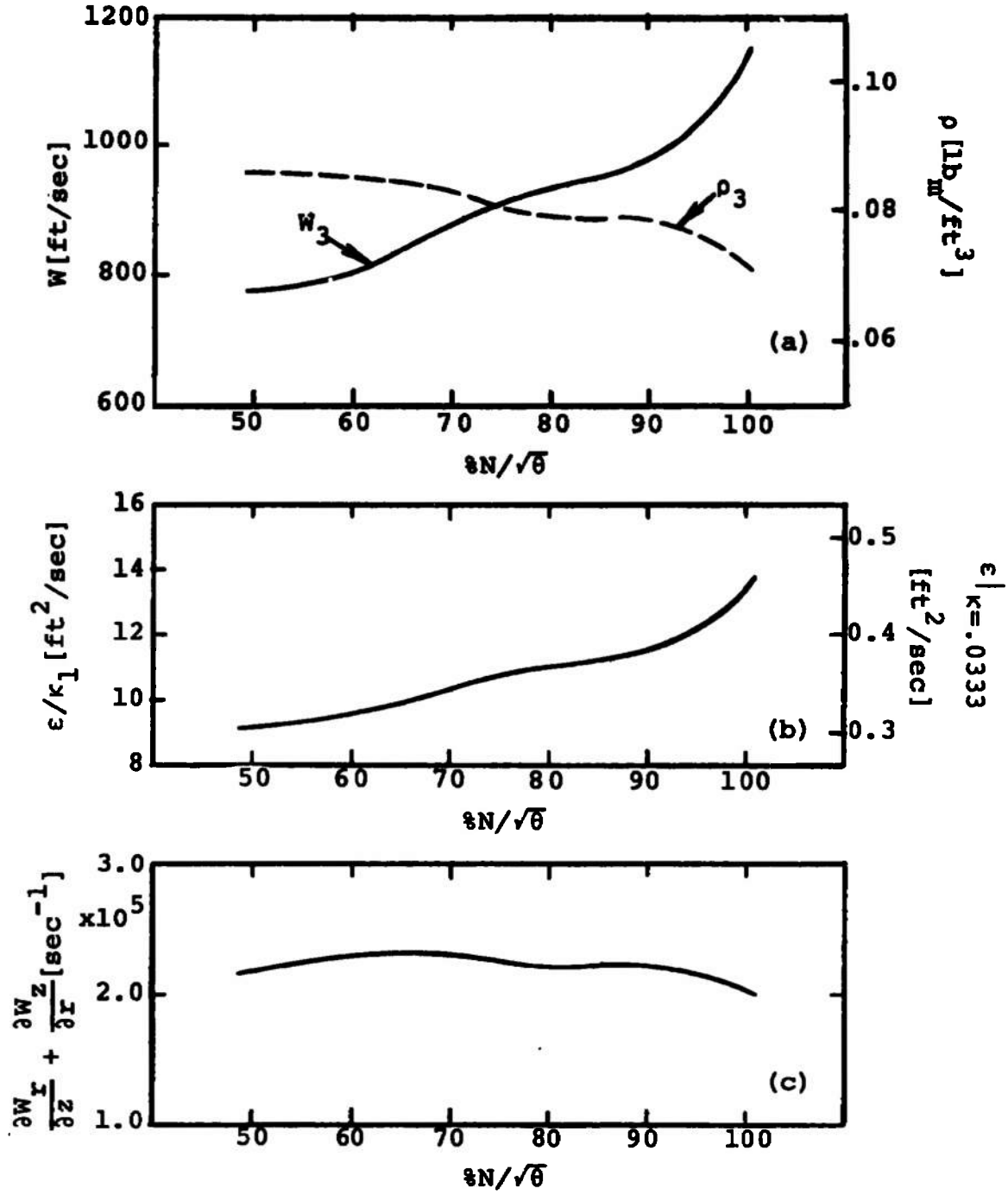


Fig. II-1 Calculated Dependence of Certain Flow Properties on Wheel Speed

Two surfaces over which shear stress must be integrated are of particular importance to the present problem. The first consists of the planes perpendicular to the axial direction. For such a plane the integrand of the shear stress integral in the momentum equation is $(-\vec{t}_z)\tau_z$ which may be resolved into radial and tangential components:

$$(-\vec{i}_z)\,\tau_z = (-\vec{a}_r)\,\tau_{zr} + (-\vec{a}_\theta)\,\tau_{z\theta} \qquad \text{(II-4)}$$

The second type of surface is the conical stream surface which bounds each streamtube. By resolving the force which produces the shear stress on this type of surface into its components, it is found that $(-\vec{t})\tau$ may be represented by

$$(-\vec{t})\tau = (-\vec{a}_r)\,\tau_{rr}\sin\xi + (-\vec{a}_\theta)\,(\tau_{r\theta}\cos\xi + \tau_{z\theta}\sin\xi) + (-\vec{k})\,\tau_{rz}\cos\xi \qquad \text{(II-5)}$$

where $\xi$ is the inclination of the stream surface with respect to axial direction measured in a plane containing the axis and where the normal stresses $\tau_{rr}$ and $\tau_{zz}$ have been neglected in the transformation.

By using Eqs. (II-4) and (II-5), the shear stress integral of the momentum equation may be written

$$\int_{(A)} (-\vec{t})\,\tau dA = (-\vec{a}_r)\left[\int_{(A_3)} \tau_{rr}\,dA_3 - \int_{(A_4)} \tau_{zr} dA_4 + \int_{(A_W)} \tau_{zr}\sin\xi\; dA_W\right]$$

$$+ (-a_\theta)\left[\int_{(A_3)} \tau_{z\theta}\; dA_3 + \int_{(A_4)} \tau_{z\theta}\, dA_4 - \int_{(A_W)} (\tau_{r\theta}\cos\xi + \tau_{z\theta}\sin\xi)\, dA_w\right]$$

$$+ (-\vec{k})\int_{(A_W)} \tau_{rz}\cos\xi\, dA_w \qquad \text{(II-6)}$$

where $A_3$ is the surface area at the blade trailing-edge plane, $A_4$ is the surface area at the downstream measuring plane, and $A_W$ represents the area of the axisymmetric surfaces bounding the streamtubes between $A_3$ and $A_4$, and where from page 54 of Ref. 13,

$$\tau_{rz} = \tau_{zr} = \rho(\nu + \epsilon)\left(\frac{\partial W_r}{\partial z} + \frac{\partial W_z}{\partial r}\right) \qquad \text{(II-7a)}$$

$$\tau_{\theta r} = \tau_{r\theta} = \rho(\nu + \epsilon)\left[r\frac{\partial}{\partial r}\left(\frac{W_\theta}{r}\right) + \frac{1}{r}\frac{\partial W_r}{\partial \theta}\right] \qquad \text{(II-7b)}$$

$$\tau_{z\theta} = \tau_{\theta z} = \rho(\nu + \epsilon)\left(\frac{1}{r}\frac{\partial W_z}{\partial \theta} + \frac{\partial W_\theta}{\partial z}\right) \qquad \text{(II-7c)}$$

The surface $A_3$ has been assumed to be located infinitesimally far upstream of the blade trailing edge. Therefore, the integral of shear stress over this surface is associated with the boundary layer on the blade profiles. Since turbulence is inhibited by the presence of solid boundaries, shear stress is expected to be less at this plane than that set up by the free turbulence occurring downstream of the rotor. For this reason, the integrals over $A_3$ will be ignored in the analysis which follows.

Consider first the radial component of Eq. (II-6). The surface $A_W$ is

$$A_W = 2\pi \int_{z_3}^{z_4} r_O(z)\,dz + 2\pi \int_{z_3}^{z_4} r_I(z)\,dz = 2\pi\Delta z\,(r_O - r_I)$$

if average values of $r_O$ and $r_I$ are selected. The largest possible value of sin $\xi$ is given by

$$\sin|\xi| < \tan^{-1}|\xi| = \frac{r_O - r_I}{\Delta z}$$

Then,

$$A_4 = \pi\,(r_O^2 - r_I^2) \approx \frac{1}{2}\sin|\xi|\,A_w$$

Thus, if an average value of $\tau_{zr}$ is selected for the entire control volume,

$$\vec{a}_r \cdot \int_{(A)} (-\vec{t})\,r\,dA \equiv f_{fr} \approx -\tau_{zr} A_4 (1 \pm 2)$$

where the sign of the shear stress integral over $A_W$ depends on the slope of the surfaces. The maximum value of this integral is then $-3\tau_{zr}A_4$. If the force due to shear stress is to cancel the resultant radial force shown in Fig. 16a, then using the values of $\rho$ and $\epsilon$ (neglecting $\nu$) shown, respectively, in Fig. II-1 top and middle and Eq. (II-7a) for $\tau_{zr}$, it is possible to estimate the magnitude of the term $(\partial W_r/\partial z + \partial W_z/\partial r)$. The result, as shown in Fig. II-1 (bottom), indicates that this term should be approximately $2 \times 10^5$ sec$^{-1}$. If such gradients occur, then $W_r$ will approach zero so that, essentially, $\partial W_z/\partial r$ alone must be on this order of magnitude. At design speed, $\partial W_z/\partial r$ is

on the order of $10^4$ in the center of the annulus at the downstream measuring plane, and it becomes much less than this as rotor speed decreases. Thus, gradients on this order (and higher, of course) are observed only in the proximity of the casing walls so some other influence must be critical.

Consider now the tangential component of Eq. (41) involving $\tau_{r\theta}$ and $\tau_{z\theta}$ as given by Eqs. (II-7b) and (II-7c), respectively. In the center portion of the annulus, $\partial W_\theta/\partial r$ may be ignored. As a first approximation, $\partial W_\theta/\partial z$ may be ignored. It must be noted that, even if the analysis demonstrates that $W_r$ becomes small in the free stream, neglecting the change of $W_r$ in the tangential direction would deny the existence of secondary radial flows which may occur in the wakes. Therefore, this term must be included in the present analysis, and the tangential component of Eq. (II-6) becomes, approximately

$$\vec{a}_\theta \cdot \int_{(A)} (-\vec{t})\tau dA \equiv f_{f\theta} \approx -\int_{(A_4)} \tau_{z\theta}\, dA_4 - \int_{(A_W)} (\tau_{r\theta}\cos\xi - \tau_{z\theta}\sin\xi)\, dA_W$$

$$\approx -\int_{(A_4)} \rho\epsilon \frac{1}{r}\frac{\partial W_z}{\partial\theta}\, dA_4 - \int_{(A_W)} \rho\epsilon\left(-\frac{W_\theta}{r}\cos\xi\right.$$

$$\left. + \frac{1}{r}\frac{\partial W_r}{\partial\theta}\cos\xi + \frac{1}{r}\frac{\partial W_z}{\partial\theta}\sin\xi\right) dA_W$$

where $\nu$ has been ignored in comparison to $\epsilon$. The term $W_\theta/r$ is neglected in comparison to the velocity change in the tangential direction. Since $\epsilon$ is of large magnitude in the wakes and negligible in the free stream, this equation reduces to

$$f_{f\theta} \approx -\frac{\rho_4\epsilon}{r}\frac{\partial W_{z4}}{\partial\theta}\, 2\pi r_{ref}\frac{b}{S}(r_0 - r_1) - 4\pi r_{ref}\int_{z_3}^{z_4}\frac{\rho\epsilon}{r}\left(\frac{\partial W_r}{\partial\theta}\cos\xi + \frac{\partial W_z}{\partial\theta}\sin\xi\right)\frac{b}{S}\, dz$$

Since

$$W^2 = W_r^2 + W_\theta^2 + W_z^2$$

then

$$\frac{\partial W}{\partial\theta} = \frac{W_r}{W}\frac{\partial W_r}{\partial\theta} + \frac{W_\theta}{W}\frac{\partial W_\theta}{\partial\theta} + \frac{W_z}{W}\frac{\partial W_z}{\partial\theta}$$

or, solving for $\partial W_r/\partial\theta$

$$\frac{\partial W_r}{\partial\theta} \approx \frac{W}{W_r}\frac{\partial W}{\partial\theta} - \frac{W_z}{W_r}\frac{\partial W_z}{\partial\theta} \qquad \text{(II-8)}$$

where it has been assumed that the chance of $W_\theta$ in the tangential direction is negligible in the wake. The result of the approximation for $\partial W_r/\partial\theta$ depends on the local value of $W_r$. It will be assumed that, in the wake, all velocity components are of comparable orders of magnitude; i.e.,

$$W^2 \approx 3W_z^2 \approx 3W_r^2 \approx 3W_\theta^2$$

Then,

$$\frac{\partial W_r}{\partial\theta} \approx 2\,\frac{\partial W_z}{\partial\theta}$$

For plane wakes at large distances from the wake producing body, Ref. 14 demonstrates that b is proportioned to $z^{\frac{1}{2}}$ and that the velocity defect varies as $z^{-\frac{1}{2}}$, so that

$$\frac{1}{r}\,\frac{\partial W_z}{\partial\theta}\,b \approx \text{constant}$$

If b may be represented by th, if

$$\frac{1}{r}\,\frac{\partial W_z}{\partial\theta} \approx \frac{W_3 - 0}{\frac{1}{2}\,r_{ref}\left(\frac{th}{r}\right)} = \frac{2\,W_3}{r_{ref}\left(\frac{th}{r}\right)}$$

and if Eq. (II-3) is used to eliminate $\epsilon$, then for constant density

$$f_{f\theta} \approx -4\pi\,\rho_3\kappa_1\,W_3^2 r_{ref}\left(\frac{th}{b}\right)\left[(r_0 - r_1) + 2\,(2\cos\xi + \sin\xi)\,(z_4 - z_3)\right]$$

$$\approx -4\pi\rho_3\kappa_1 W_3^2 r_{ref}\left(\frac{th}{b}\right)\left[1 + 1\,(2\cos\xi + \sin\xi)\right](1\text{ in.}) \qquad \text{(II-9)}$$

since

$$r_0 - r_1 \approx 1\text{ in.}$$
$$z_4 - z_3 \approx 2\text{ in.}$$

Equation (II-9) shows that integration of the shear stress over the stream surfaces is quite important. By assuming that $\xi$ is small, commensurate with small values of $W_r$ in the free stream, then $f_{f\theta}$ becomes

$$f_{f\theta} \approx -36\,\pi\rho_3\kappa_1 W_3^2 r_{ref}\left(\frac{th}{9}\right)(1\text{ in.})$$

The results of the calculation of the absolute magnitude of the force due to friction in the tangential direction ($f_{f\theta}$) are shown in Fig. II-2 where the computations have used $\rho_3$ and $W_3$ given in Fig. II-1a,

$$\kappa_1 = 0.0333$$

$$r_{ref} = 20.450 \text{ in.}$$

$$\frac{th}{s} = 0.272$$

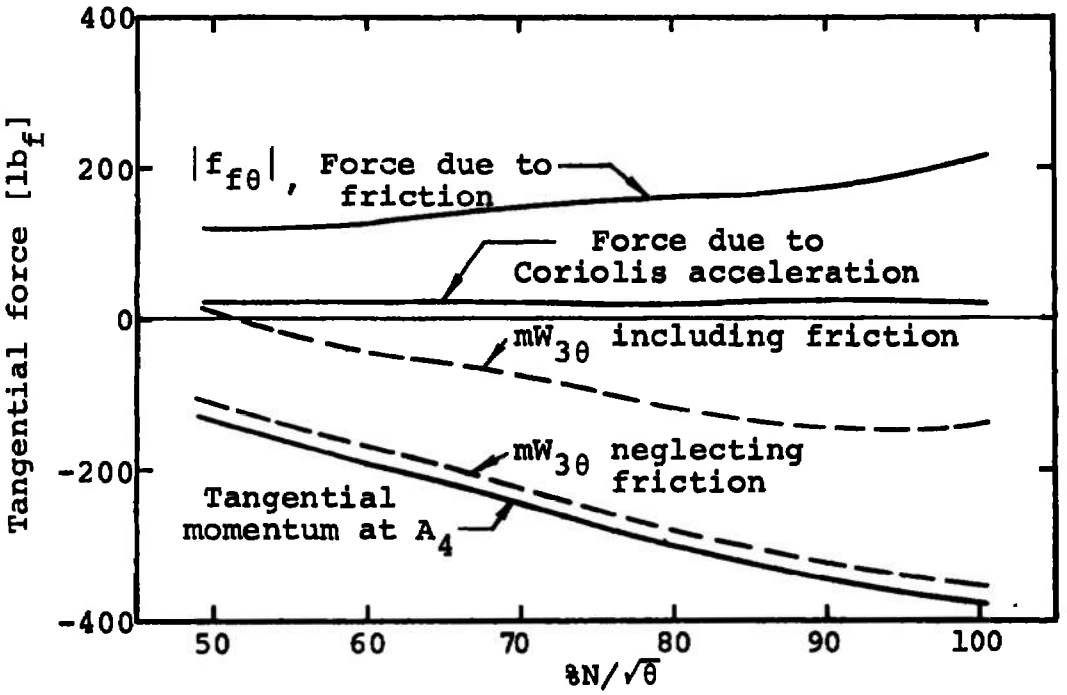


**Fig. II-2 Comparison of Forces Affecting the Tangential Component of the Momentum Equation**

Consider the following simplified form of the tangential component of the momentum equation neglecting unsteady effects and the weight of the gas:

$$mW_{4\theta} - mW_{3\theta} = f_{f\theta} - f_{Coriolis\theta}$$

or, solving for $W_{3\theta}$ while noting $W_{4\theta}$ and $f_{f\theta}$ are negative in the present case,

$$W_{3\theta} = \frac{1}{m}\left(f_{Coriolis\theta} - m|W_{4\theta}| + |f_{f\theta}|\right) \qquad \text{(II-10)}$$

The tangential components of the force due to Coriolis acceleration and of the quasi-two-dimensional average momentum passing through $A_4$ are also shown in Fig. II-2 in relation to this equation. It is seen from Eq. (II-10) that the addition of the tangential frictional forces will cause

$W_{3\theta}$ to be less negative. This is indicated in Fig. II-2 by the differences between the tangential momentum at $A_3$ calculated by neglecting friction and by the inclusion of the frictional force. Since the radial component of Coriolis acceleration depends on $W_\theta$, the neglection of friction implies an overestimation of the radial force due to Coriolis acceleration.

It is noted that, if $W_r$ is decreased by the addition of friction, then the tangential force due to Coriolis acceleration is also reduced and that, if $W_{3\theta}$ is reduced, it is possible that the good agreement between the present solution for $\beta_3$ and the blade angle may be destroyed. Both of these factors are fundamentally dependent on the coupling of the components of the momentum equation through, not only the Coriolis acceleration term which connects the radial and tangential components, but also the introduction of friction which connects all three components. The effects of coupling make the final result extremely difficult to predict, but it is felt that the tendency toward correction of the present solutions has been satisfactorily demonstrated.

UNCLASSIFIED

Security Classification

**DOCUMENT CONTROL DATA - R & D**

*(Security classification of title, body of abstract and indexing annotation must be entered when the overall report is classified)*

| 1 ORIGINATING ACTIVITY (Corporate author) | 2a. REPORT SECURITY CLASSIFICATION |
|---|---|
| Arnold Engineering Development Center, ARO, Inc., Operating Contractor, Arnold Air Force Station, Tennessee 37389 | UNCLASSIFIED |
| | 2b. GROUP N/A |

3 REPORT TITLE

AN APPROXIMATE SOLUTION OF THE SUDDEN AREA EXPANSION FLOW PROCESS FOR FLOWS IN A ROTATING COORDINATE SYSTEM

4 DESCRIPTIVE NOTES (Type of report and inclusive dates)

December 1968 to December 1969 - Final Report

5. AUTHOR(S) (First name, middle initial, last name)

J. W. Salvage, ARO, Inc.

| 6 REPORT DATE | 7a. TOTAL NO. OF PAGES | 7b. NO OF REFS |
|---|---|---|
| August 1971 | 86 | 15 |

| 8a. CONTRACT OR GRANT NO F40600-72-C-0003 | 9a. ORIGINATOR'S REPORT NUMBER(S) |
|---|---|
| b. PROJECT NO 7065 | AEDC-TR-71-111 |
| c. Program Element 6144501F | 9b. OTHER REPORT NO(S) (Any other numbers that may be assigned this report) ARO-ESF-TR-70-330 |
| d. | |

10 DISTRIBUTION STATEMENT

Approved for public release; distribution unlimited.

| 11. SUPPLEMENTARY NOTES | 12. SPONSORING MILITARY ACTIVITY |
|---|---|
| Available in DDC. | Aerospace Research Laboratories, Air Force Systems Command, Wright-Patterson AFB, Ohio 45433. |

13 ABSTRACT

An approximate quasi-three-dimensional method of solution is described for the sudden area expansion flow process in the relative coordinate system under the assumptions of frictionless, adiabatic flow of a perfect gas. The objective was to determine the radial variation of the flow properties at the trailing edge of a rotor given the measured flow properties downstream of the rotor through use of the streamtube approximation. Results are derived from one configuration of the blunt trailing-edge supersonic compressor rotors tested at AEDC. The results were felt to be an unsatisfactory representation of the average flow conditions at the trailing edge, and it is shown that the reasons for this are relatable to neglecting the free turbulent shear flows occurring in the blade wakes in conjunction with neglecting the large radial secondary flows which apparently occur in the flow field of the rotor investigated. It is shown that the streamtube approximation can produce grossly inaccurate results when free turbulent shear is neglected on the streamtube boundaries. A proposal for continued work is also given.

DD FORM 1 NOV 65 1473

UNCLASSIFIED

Security Classification

| 14. KEY WORDS | LINK A | | LINK B | | LINK C | |
|---|---|---|---|---|---|---|
| | ROLE | WT | ROLE | WT | ROLE | WT |
| axisymmetric flow | | | | | | |
| flow process control | | | | | | |
| three-dimensional flow | | | | | | |
| two-dimensional flow | | | | | | |
| adiabatic flow | | | | | | |
| trailing edges | | | | | | |
| supersonic flow | | | | | | |
| compressor rotors | | | | | | |
| compressor blades | | | | | | |
| equations of state | | | | | | |